

SSRMP Annual Scientific Meeting 2015

Fribourg, 21st and 22nd October 2015



Schweizerische Gesellschaft für Strahlenbiologie und Medizinische Physik
Société Suisse de Radiobiologie et de Physique Médicale
Società Svizzera di Radiobiologia e di Fisica Medica
Swiss Society of Radiobiology and Medical Physics

SGSMP
SSRPM
SSRFM

Plan to perform

Flexitron

Flexitron® delivery with Oncentra® Brachy planning



When Oncentra treatment planning (v 4.5) is used in combination with the new Flexitron afterloading platform, you will optimally benefit from a number of smart features that allow an easy, standardized way of treatment planning – while feeling confident about accurate and safe treatment delivery. Benefit from constant settings, such as a fixed step size and a fixed length for transfer tubes (1000 mm). The friendly user-interface helps you save time.

View the Plan to Perform video on elekta.com/flexitron

888.00692 MKT [00]

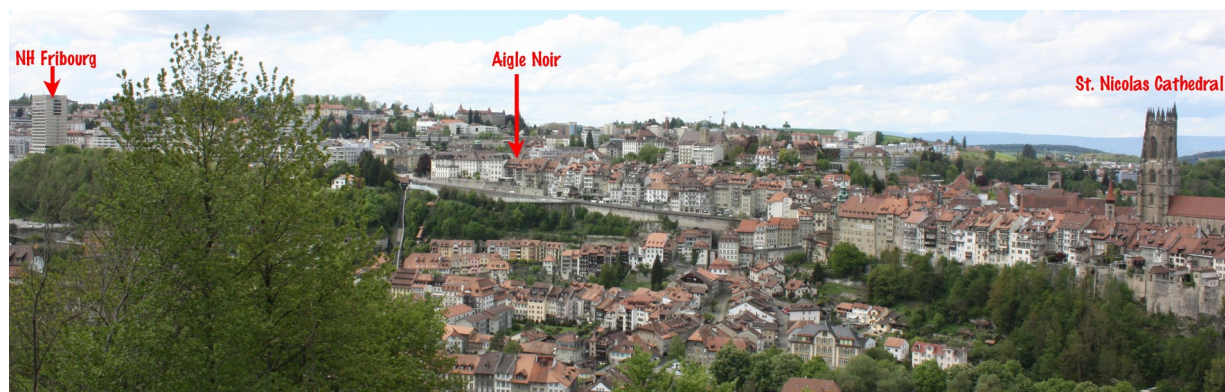
More at elekta.com



SSRMP Annual Scientific Meeting 2015

Fribourg, 21st and 22nd October 2015

| | |
|-----------------------|--|
| Venues | NH-Hotel, Fribourg Grand-Places 14 CH-1700 Fribourg |
| Contact | Pierre-Alain Tercier +41 26 4267681 Pierre-Alain.Tercier@h-fr.ch |
| Organizing Committee | Frédéric Miéville Olivier Pisaturo Pierre-Alain Tercier |
| Scientific Committee | Shelley Bulling, Genève Michael Fix, Bern Frédéric Miéville, Fribourg Marc Pachoud, Vevey Olivier Pisaturo, Fribourg Pierre-Alain Tercier, Fribourg |
| Scientific Program | Wednesday 21st October 2015, 10:15-16:00 Thursday 22nd October 2015, 8:30-16:30 |
| Lunch Sponsors | Varian, and Accuray |
| Apero Sponsors | Elekta and RaySearch |
| Evening Events | Apero at 18:00 at NH Hotel, Fribourg Conference dinner 19:30 at Restaurant « L'Aigle Noir », Fribourg (5 minutes from NH-Hotels) |
| Industrial Exhibition | NH-Hotel, in front of conference room |



Welcome at Fribourg

On behalf of the local organizing committee it is a pleasure to welcome you to the Annual Scientific Meeting 2015 of the SSRMP at the NH-Hotel in Fribourg.

The scientific program covers again the whole range of the community : the sessions will inform you of the status and new developments in dosimetry and radioprotection, quality assurance and dose calculation, nuclear medicine, dosimetry and dosimetric verification, as well as diagnostics.

Coffee breaks and lunch will be served on the same floor as the conference together with the industrial exhibition, and we invite you to an aperitif after the first day between 18:00 and 19:15. The conference dinner will take place the 21st October at 19:30 at the Restaurant « Aigle Noir » in Fribourg.

We hope you enjoy this annual event of the SSRMP and wish you an inspiring scientific meeting.

Pierre-Alain Tercier

Program

Wednesday, October 21

- 9:00-10:00 Registration and Coffee
- 10:00 Opening ceremony
- 10:15-12:00 Session 1 : Radioprotection
- 12:00-13:15 Lunch break sponsored by Varian
- 12:30-13:15 Industrial exhibition
- 13:15-14:45 Session 2: Advanced Imaging
- 14:45-16:00 Session 3: Motion management
- 16:00-16:30 Coffee break and poster session
- 16:30-18:00 General Assembly SSRMP
- 18:00-19:15 Apéro (NH-Hotel), sponsored by Elekta and RaySearch
- 19:30 Conference dinner (Restaurant « Aigle Noir »)

Thursday, October 22

- 8:30-10:00 Session 4: Radiotherapy I
- 10:00-10:30 Coffe break and posters session
- 10:30 Special Session : Importance of a quality management system in a department of radiation oncology
- 11:30-12:45 Lunch break sponsored by Accuray
- 12:00-12:45 Industrial exhibition
- 12:45-14:45 Session 5 : Radiotherapy II
- 14:30-15:00 Coffee break and posters session
- 15:00-16:30 Session 5 : Radiotherapy III
- 16:30 Closing

Industrial Exhibition

Accuray

BrainLab

ConMedica

Elekta

Meditron

Qualiformed

Philips AG Healthcare

PTW

Solumedics GmbH

Raditec Medical AG

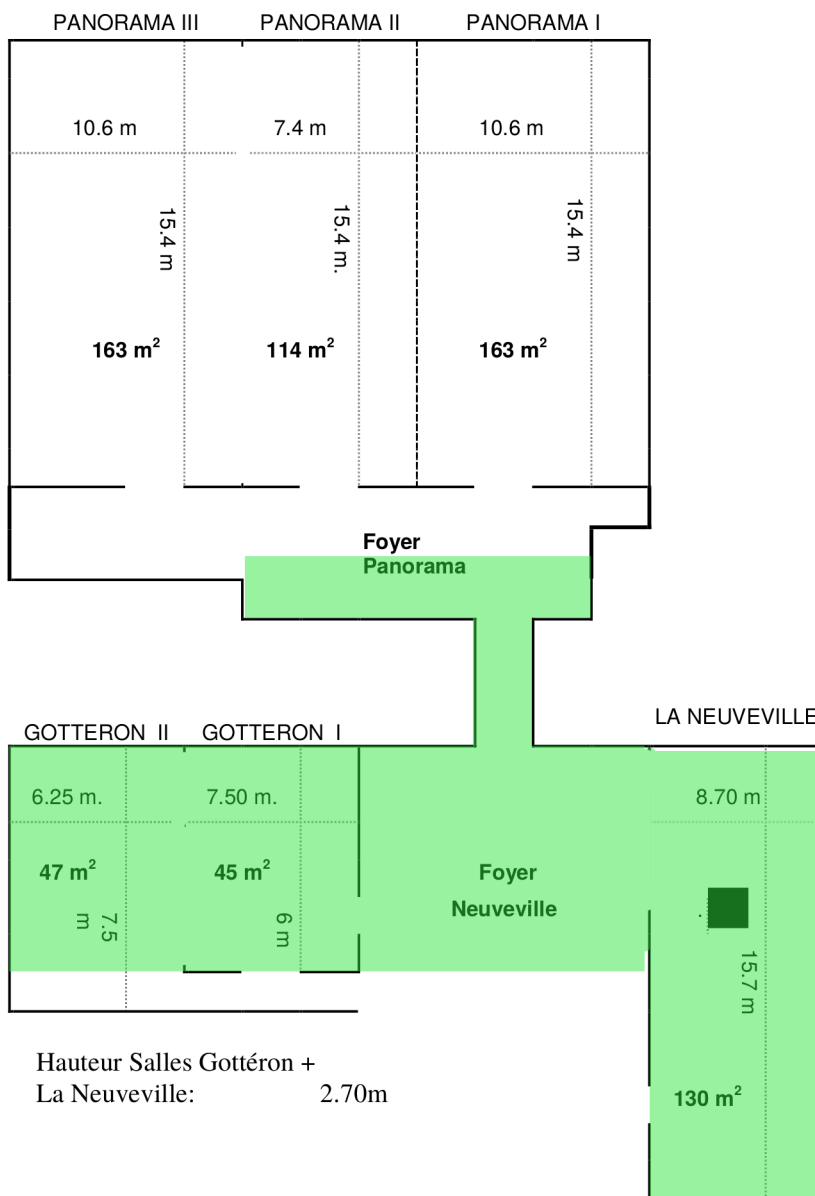
RaysearchLabs

Roentgen AG

Varian

Niveau -1

Hauteur Salles Panorama : 3.53m



Scientific Program

Wednesday, October 21

9:00 – 10:00 Registration and Coffee

10:00 **Opening ceremony**
Peter Manser, SSRMP President

Session 1 : Radioprotection (*Buchauer K. and Pempler P.*)

10:15 – 12:00

10:15 **Linac activation of radioisotopes and underground gammaspectroscopic analyses**
P. Weber, G. Guibert, C. Tamburella

10:30 **Measurement and Monte Carlo Calculation of Organ Doses for Digital Volumetric Tomography**
M. Ernst, M. K. Fix, P. Manser, K. Dula

10:45 **Standardized Quality Assessment Protocol for Implementation of Art.74 in Nuclear Medicine.**
G. Di Domenicantonio, S. Gnesin, T. Lima

11:00 **Optimization of the planning CT-scans in radiation oncology: An image quality based approach**
N. Ryckx, N. Ruiz Lopez, R. Moeckli, F. R. Verdun

11:15 **Dose Optimization and Radiation Protection in Interventional Radiology using Real-Time Dosimetry**
J. Binder, N. Icken, T. V. M. Lima, I. Özden, G. Lutters

11:30 **Evaluation of Patients Dose in PET Studies from CT Contrast Agents**
T.V.M. Lima, J. Binder, I. Oezden, K. Strobel, S. Matijasevic, A. Bopp, E. Nitzsche, G. Lutters

11:45 **The Use of Dose Length Product DLP, Signal-to-Noise Ratio SNR and Difference Detail Curve DDC for CT Protocol Characterization and Optimization**
I. Oezden, C. Sommer, G. Lutters, S. Scheidegger

Lunch break sponsored by Varian

12:00 – 13:15

Industrial exhibition

12:30 – 13:15

Session 2: Advanced Imaging (*Miéville F. and Vetterli D.*)

13:15 – 14:45

- 13:15** **New trends in biomedical imaging using atomic magnetometers**
Invited speaker : Antoine Weis, University of Fribourg
- 14:00** **Numerical simulation of X-ray grating interferometry imaging using Monte Carlo methods**
S. Peter, M. K. Fix, P. Manser, M. Stampanoni
- 14:15** **Task-based assessment of a the novel ADMIRE algorithm**
J. G. Ott, A. Ba, D. Racine, N. Ryckx, F. O. Bochud, F. R. Verdun
- 14:30** **Texture analysis of CT perfusion maps – stability study**
M. Nesteruk, R. Bundschuh, O. Riesterer, P. Veit-Haibach, G. Studer, S. Stieb, S. Glatz, H. Hemmatazad, G. Huber, M. Pruschy, M. Guckenberger, S. Lang

Session 3: Motion management (*Fix, M. and Moeckli R.*)

14:45-16:00

- 14:45** **Intra- and interfraction motions assessed with Cone-Beam CT and fluoroscopy for lung SBRT**
C. Castella, T. Breuneval, P. Tsoutsou
- 15:00** **Modeling of a Robotic Treatment Table to improve the Control Performance**
M. Stäuble, A. Jöhl, M. Schmid Daners, M. Meboldt, S. Klöck, M. Guckenberger, S. Lang
- 15:15** **A comparison of different respiratory motion management techniques**
S. Ehrbar, R. Perrin, M. Peroni, K. Bernatowicz, T. Parkel, D. Ch. Weber, A. Lomax, I. Pytko, S. Klöck, M. Guckenberger, S. Lang
- 15:30** **Dosimetric Impact of Geometric Uncertainties in Navigated HDR-Brachytherapy for Liver Tumors**
L. Witthauer, S. Weber, D. Terribilini, M.K. Fix
- 15:45** **Feasibility study of using a radiofrequency tracking system for intra-fractional monitoring during radiosurgery**
I. Pytko, A. Stüssi, S. Lang, S. Klöck, M. Guckenberger

16:00 – 16:30 Coffee break and poster session

16:30 – 18:00 General Assembly SSRMP

18:00 – 19:15 Apéro sponsored by Elekta and Raysearch Inc.

19:30 **Conference dinner**

Thursday, October 22

Session 4: Radiotherapy I (*Thengumpallil S. and Castella C.*)

8:30-10:00

- 8:30** **A dosimetric comparison of MERT and mixed beam therapy for selected head and neck tumors**
A. Joosten, S. Müller, D. Henzen, W. Volken, D. Frei, D.M. Aebersold, P. Manser, M.K. Fix
- 8:45** **Knowledge based planning model assessment for breast VMAT planning**
A.Fogliata, C.Bourgier, F.DeRose, P.Fenoglietto, F.Lobefalo, P. Mancosu, S.Tomatis, M.Scorsetti, L.Cozzi
- 9:00** **A clinical distance measure for evaluating radiotherapy treatment plan quality difference with Pareto fronts**
K. Petersson, A. Kyroudi, J. Bourhis, F. Bochud, and R. Moeckli
- 9:15** **Monte Carlo Based Analysis of Dose Rate Distributions in Volumetric Modulated Arc Therapy**
P.-H. Mackeprang, W. Volken, D. Terribilini, D. Frauchiger, K. Zaugg, D.M. Aebersold, M.K. Fix, P. Manser
- 9:30** **A comparison of 6 planning RT techniques for breast treatments**
M.Zeverino, N. Ruiz Lopez, M. Marguet, W. Jeanneret Sozzi, J. Bourhis, F. Bochud, R. Moeckli
- 9:45** **A clinical protocol for Simultaneous Integrated Boost for proton treatment**
MF Belosi, R Malyapa (MD), A Bolsi, AJ Lomax, DC Weber (MD)

10:00 – 10:30 Coffe break and posters session

Special session : (*Tercier P.-A.*)

- 10:30** **Importance of a quality management system in a department of radiation oncology**
Invited speaker, Alain Najjar

Lunch break sponsored by Accuray

11:30-12:45

Industrial exhibition

12:00-12:45

Session 5 : Radiotherapy II (*Seiler R. and Moeckli R.*)

12:45-14:45

- 12:45** **Improving lateral penumbra using contour scanned proton therapy**
Gabriel Meier, Dominic Leiser, Rico Besson, Alexandre Mayor, Sairos Safai, Damien Charles Weber, Antony John Lomax
- 13:00** **TransitQA – Concept of transit dosimetry for Tomotherapy treatments**
O. Pisaturo, F. Miéville, P-A. Tercier, A.S. Allal
- 13:15** **A general model of stray dose calculation of static and intensity-modulated photon radiation beams**
P.Hauri, Roger A. Hälgl, J.Besserer, and Uwe Schneider
- 13:30** **A novel approach to the reference dosimetry of proton pencil beams based on dose-area product**
C. Gomà, B. Hofstetter-Boillat, S. Safai, S. Vörös
- 13:45** **Comparison of various dosimeters at high dose-rate**
M. Jaccard, K. Petersson, C. Bailat, T. Buchillier, J. Bourhis, R. Moeckli, F. Bochud
- 14:00** **3d printed dose compensation body to remove dose artifacts of a HDR Brachytherapy surface applicator of the vertical type.**
K. Buchauer, L. Plasswilm, H. Schiefer
- 14:15** **Research Activities at the Bern Medical Cyclotron**
M.Auger, S.Braccini, T.S.Carzaniga, A. Ereditato, K. Nesteruk, P. Scampoli
- 14:30-15:00** **Coffee break and posters session**
- Session 5 : Radiotherapy III (Bulling S. and Manser P.)**
- 15:00-16:30**
- 15:00** **Changing from ITV to MidV concept – Do we have to increase the prescribed dose?**
A. Tartas, S. Ehrbar, L. S. Stark, M. Guckenberger, S. Klöck, S. Lang
- 15:15** **Proton radiography for the clinical commissioning of the new Gantry2 head support at PSI**
L. Placidi, S. König, R. van der Meer, F. Gagnon-Moisan, A. J. Lomax, D. C. Weber, A. Bolsi
- 15:45** **StereoPHAN™, an end-to end phantom for SBRT**
F. Hasenbalg, T. Buchsbaum, C. Erckes, K. Haller and P. Pemler
- 16:00** **A Novel Approach of Customized Shielding in Superficial and Orthovoltage Radiotherapy**
M. Baumgartl, A. Dietschy, K.S. Bertapelle, Dr. S. Hemm-Ode, A. Pfäfflin, Dr. G. Kohler
- 16:15** **Evaluation of Machine Performance Check**
M. Zamburlini, I. Pytko, A. Stüssi, T. Rudolf, S. Klöck, S. Lang
- 16:30** **Closing**

Posters

List of posters presentation

- (P01) **Variability of PET image noise as function of acquisition and reconstruction parameters and its usefulness for quantifying tumor hypoxia**
R. Kueng , P. Manser , M. Fix , H. Keller
- (P02) **MC Simulation of Electron Transport in Homogeneous Magnetic Fields: Dosimetric Effects for MeV Electron Beams**
S. Höfel, D. Frei, P. Manser, M.K. Fix
- (P03) **On the RapidArc commissioning tests by Ling et al. 2008: the IOSI experience with old and new tests.**
G. Nicolini, A. Clivio, E. Vanetti
- (P04) **The Current Status of the Implementation of Clinical Audits in Switzerland**
M. Gasser, R. Treier, Ph. R. Trueb
- (P05) **An adequate Quality Assurance technique for superficial hyperthermia equipment**
G. vanStam, D. Marder, M. Capstick, O. Timm, G. Lutters
- (P06) **A method for pre-treatment verification of hyperthermia treatment plans**
D.Marder, N.Brändli, G.vanStam and G.Lutters
- (P07) **Comparison of Image Quality and Radiation Exposure between Dental Volume Tomography DVT and Conventional CT by Using a Novel Skull – DLP Phantom**
C. Sommer, I. Oezden, G. Lutters, A. Cornelius, S. Scheidegger
- (P08) **Comparative patient dosimetric estimates for different radiological facilities when performing maxillofacial examinations**
Marta Sans-Merce, Jérôme Damet, Minerva Becker
- (P09) **Verification and validation of a cylindrical 3D water scanner**
T. Götzfried, A. von Deschwanden

Linac activation of radioisotopes and underground gammaspectroscopic analyses

P. Weber, G.Guibert, C.Tamburella

Hôpital neuchâtelois, Service de radiothérapie du DPO

Introduction

After irradiating various linac parts with photon beams, we performed underground gammaspectroscopic measurements of the samples only a few minutes after the irradiation, in order to observe short-lived radioisotopes.

Materials and Methods

Three samples were used : a new flattening filter (never irradiated before), an old flattening filter, unmounted from a linac in 2012 and an old tungsten leaf. All the samples were measured in the underground laboratory of la Vue-des-Alpes, equipped with an ultralow noise germanium detector, before the irradiations.

The new flattening filter and the leaf were then irradiated with 200Gy under 15MV and 6MV photon beams. The gamma counting began 20 minutes after the irradiations. A GEANT4 simulation was run for every samples, allowing quantitative results of the measured activity.

Results

A residual activity of 236.9Bq was measured in the old filter with long-lived radioisotopes, such as ^{57}Co , ^{54}Mn and ^{60}Co . Before irradiation, the old tungsten leaf and the new filter gamma counting showed only tiny amounts of ^{238}U , ^{57}Co , ^{54}Mn and ^{60}Co , with a total activity of 0.51 and 0.02Bq, respectively. Irradiations with 15MV led to (n, γ) activation of short-lived isotopes : In the leaf, the measured activity was 1556 Bq just after the irradiation and we observed various gamma lines from ^{187}W , ^{57}Ni and ^{56}Mn . In the new filter, the activity was 1097Bq and the gamma signature of ^{56}Mn , ^{56}Ni , ^{57}Ni and ^{59}Co was clearly present. Irradiations at 6MV led to a very small activation of radioisotopes. Gammaspectroscopic data was taken several times after the irradiation to monitor the time evolution and the total activity.

Conclusion

Treating patients with 15MV photon beams activate long-lived radioisotopes in the linac head. With this work, it was possible to identify these isotopes, but the goal was especially to highlight the short-lived radioisotopes created.

Measurement and Monte Carlo Calculation of Organ Doses for Digital Volumetric Tomography

M. Ernst (1), M. K. Fix (2), P. Manser (2), K. Dula (3)

(1) Radiotherapy Hirslanden, Witellikerstrasse 40, Zurich, Switzerland

(2) Division of Medical Radiation Physics and Department of Radiation Oncology, Inselspital, Bern University Hospital, and University of Bern, Switzerland

(3) Zahnmedizinische Klinik, Inselspital, Bern University Hospital, and University of Bern, Switzerland

Introduction

In dentistry the use of cone beam CT (CBCT) is known as Digital Volumetric Tomography (DVT) and its use has steadily increased over the last few years. The aim of this study was to measure organ doses and to compare it with dose calculations based on Monte Carlo (MC) simulations.

Materials and Methods

LiF detectors TLD-100 were placed at 71 measurement positions within and on the surface of an anthropomorphic phantom to cover all relevant radiosensitive organs and tissues. Protocols specific for three different examinations were performed on a 3D Accuitomo 170 (J. MORITA MFG. CORP.). Dose calculations with MC simulation were performed for the same three protocols using the EGSnrc transport code system.

Results

Mean of organ doses for the three protocols ranged from 5.2 mGy (FOV 140x100 mm²) to 2.75 mGy (FOV 80x50 mm²) and 1.5 mGy (FOV 40x40 mm²). An overall accuracy of $\pm 50\%$ for the MC calculation of organ doses with respect to the TLD measurements was achieved.

Conclusion

The dose values of a DVT machine are indeed lower than the one of a conventional CT examination, but can be about 20 times higher than the dose values of a panoramic dental examination. CBCT should therefore be reserved for complex cases where its application can be expected to provide further information that is relevant to the choice of therapy. In this study, the bases for the application of the MC method for dose determination of DVT were examined, but further studies need to be performed.

Standardized Quality Assessment Protocol for Implementation of Art.74 in Nuclear Medicine

G. Di Domenicantonio(1), S. Gnesin(2), T. Lima(3)

(1) *Hôpitaux Universitaires de Genève, Department of Nuclear Medicine and Molecular Imaging*

(2) *Institute of Radiation Physics, Lausanne University Hospital*

(3) *Kantonsspital Aarau AG, Department of Radiation Protection*

Introduction

In the framework of the application of the Swiss Radiological Protection Ordinance (SRPO) of 22 June 1994 and, in particular, of the 'Art.74' in Nuclear Medicine, the authors are presenting the implementation of a measurement protocol to be used for standardized quality assessment tests and for dose optimization purposes in PET and SPECT medical imaging.

Materials and Methods

Standard phantoms (NEMA-NU2 and Jaszczak) are filled with typical clinical activity concentration (5MBq/l for PET and 10MBq/l for SPECT) and scanned with different acquisition times. Standard image quality descriptors (RC, COV) are extracted in order to evaluate detectability and signal recovery as a function of spheres' size lesion contrast and background noise level.

Results

Preliminary results on 8 PET scanners and 8 SPECT scanners are presented. The physicist's involvement (time required for data acquisition and analysis) has been evaluated. A procedure for setting a window of acceptability for image quality values is described and applied to preliminary results.

Conclusion

The authors believe that the proposed protocol could be adopted for the implementation of the NM part of Art. 74 of the SRPO. The protocol will also facilitate the harmonization of quality assessment procedures at a national level and allow for inter-center data-sharing.

Optimization of the planning CT-scans in radiation oncology: An image quality based approach

N. Ryckx(1), N. Ruiz Lopez(1), R. Moeckli (1), F. R. Verdun (1)

(1) *Lausanne University Hospital, Institute of Radiation Physics*

Introduction

The introduction of an automatic dose collection software (DoseWatch, GE Healthcare) raised awareness about high cumulative patient doses due to planning CT in the radiation oncology (RO) department. Furthermore, the recent arrival of a Cyberknife (CK) treatment system (Accuray) called for planning CT protocols with high technical parameters. As a consequence, dose-length products (DLP) of several tens of Gy cm were not uncommon. This contribution presents the first steps in the optimization of planning CT-scanners at our institution.

Materials and Methods

The CT used for treatment planning is a Toshiba Aquilion LB. The first step was to verify the accuracy of the dose indicators (CTDIvol and DLP) using the standard CTDIvol (16 and 32 cm PMMA cylindrical) phantoms and a 100 mm pencil ionization chamber (Radcal). Then, two image quality (IQ) phantoms (Catphan 600 and QRM abdomen hull with low-contrast lesions) were scanned using the standard RO and CK protocols and analyzed respectively for spatial resolution and low contrast detectability (LCD). Patient doses for 2014 and 2015 were analyzed using DoseWatch to bring out optimization starting points. Finally, an anthropomorphic phantom with built-in tumor (CIRS 4D) was scanned using the original CK protocol and the same protocol with automatic exposure control (AEC). The DRR generated by the TPS were then compared using ImageJ and Matlab.

Results

The indicated CTDIvol corresponds to the maximum CTDIvol issued during the acquisition phase - and not the average CTDIvol. However, the DLP is calculated integrally is thus correct. Standard RO protocols have an image quality suitable for planning and correspond to clinical requirements. The CK protocols, however, show an IQ way above the average. Finally, the creation of DRR for CK treatment shows no significant difference between the native technical parameters or the scans using the AEC system, thus showing a potential dose reduction per planning CT for the CK protocols.

Conclusion

A multiple tool approach was used in order to start the optimization of the RO and CK planning CT scans, especially the latter. Some minor elements could be immediately corrected. A report was established and submitted to the RO department for approval.

Dose Optimization and Radiation Protection in Interventional Radiology using Real-Time Dosimetry

J. Binder, N. Icken, T. V. M. Lima, I. Özden, G. Lutters;

Kantonsspital Aarau, Fachstelle Strahlenschutz, Aarau/CH

Introduction

Medical staff in x-ray supported interventions is among the professionals most highly exposed to ionizing radiation. To avoid the limitations of long term averaging inherent in the legally required TLD personal dosimeters and gain better insight into the circumstances of high exposure rates studies using a real-time dose reporting and recording system were performed and analyzed considering the achievable limit of staff exposure reduction.

Materials and Methods

The dosimetry system consisted of solid-state detectors carried by each participant over the protective apron which were connected wirelessly to a real-time display also offering the opportunity of reviewing the received dose rate curves. Simultaneously all interventions were recorded in time-synchronized videos. These were retrospectively analyzed to identify significant exposure situations and find reasons. Besides the total dose was protocolled together with intervention dose parameters. Based on this learning sessions on radiation protection for the IR team were held presenting the results and important findings.

Results

Observations in more than 100 interventions in 5 interventional radiology and angiology, 2 neuroradiology, 5 cardiology, 2 gastroenterology and 2 urology suites are reported showing very widespread distributions with standard deviations not rarely of 100% in cumulative dose, fluoroscopy time and dose area product even in equal procedure types.

Conclusion

Obviously poor or inadequate radiation protection equipment on site impeded low exposure and imprudent handling gave raise to unnecessary organ doses especially to eyes.

Conversely a concerned and well trained use of the equipment, careful selection of imaging protocols, predominant use of fluoroscopy modes and retrospective appraisal can significantly reduce the dose to patient and staff.

Evaluation of Patients Dose in PET Studies from CT Contrast Agents

T.V.M. Lima (1,2,3), J. Binder (1), I. Oezden (1), K. Strobel (4), S. Matijasevic (4), A. Bopp (5), E. Nitzsche (5), G. Lutters (1)

(1) *Fachstelle Strahlenschutz, Kantonsspital Aarau AG, Aarau, Switzerland*

(2) *Life Science Section, CERN - European Organization for Nuclear Research, Geneva, Switzerland*

(3) *Division of Surgery and Interventional Science, University College London, London, UK*

(4) *Nuklearmedizin, Luzerner Kantonsspital, Luzern, Switzerland*

(5) *Nuklearmedizin, Kantonsspital Aarau AG, Aarau, Switzerland*

Introduction

The increased availability of PET-CT devices in addition to the interchange of people and technology between nuclear medicine and radiology explains the increased use of CT techniques like enhanced contrast CT in nuclear medicine. The benefits of the use of contrast agents, especially in terms of the increased accuracy, for enhancing different image modalities are understood and well discussed in the literature. On the other hand, in terms of evaluating the different side effects from the use of these contrast agents only the visible and short-term reactions have been discussed. In respect to studying for a possible increase in dose exposure from the interaction of the radiopharmaceutical radiation with the contrast agent in a contrast enhanced PET-CT study and its effect in the patient radiation exposure is yet to be investigated.

Materials and Methods

This study is aimed to investigate the dose deposition differences with respect to the nuclear medicine isotope radiation interaction with the high density and atomic number of the contrast agent due to increased absorption and scatter of the internal radiation in the patients' tissue. This has been performed with the use of Monte Carlo simulations of 10 patient studies where contrast agent had been used.

Results

Preliminary results show an increase in the dose deposition in the regions enhanced by contrast and its surroundings.

Conclusion

Further quantification of this increased dose deposition in different organs at risk and its estimated effect will be presented.

The Use of Dose Length Product DLP, Signal-to-Noise Ratio SNR and Difference Detail Curve DDC for CT Protocol Characterization and Optimization

I. Oezden(1), C. Sommer(2), G. Lutters(1), S. Scheidegger(1,2)

(1) *Kantonsspital Aarau, Institute of Radiation Oncology*

(2) *ZHAW School of Engineering*

Introduction

For evaluation of CT protocols in clinical routine, different CT units from four manufactures have been characterized by simultaneous measurements of dose length product DLP and image quality parameters by using the elliptical ZHAW phantom.

Materials and Methods

The elliptical ZHAW Phantom is built on PMMA slabs with different effective diameter (32 cm corresponding to the standard CTDI body phantom and 19/22/28 cm) containing different elements for measuring SNR, contrast-to-noise ratio CNR and modulation transfer function MTF. In addition, we developed a Difference-Detail-Curve (DDC) phantom using NaCl-and contrast-media solutions with different concentrations. The analysis is carried out by dedicated software, allowing the calculation of SNR and CNR through the image stack as function of slice position. The DLP is measured according the standard CTDI phantom (10cm- and 30 cm- chamber in central and peripheral positions).

Results

The DDC-method delivers relevant information about low contrast detectability in a very intuitive way whereas it was difficult to derive a meaningful interpretation for CNR values. Regarding the measured DLP, CTDI and SNR, a clear potential of optimization concerning automatic exposure control (AEC) was found: In some cases, a smaller pitch value resulted in a lower DLP due to a higher resolution of the tube current regulation and reduced over-scanning.

Conclusion

Based on our experience, the DDC-method should be used instead of CNR for evaluation of low contrast detectability. SNR can be used in combination with the tube current information available for every rotation to get a detailed insight into the dynamic behavior of AEC, especially when combining phantom slabs with different effective diameters.

New trends in biomedical imaging using atomic magnetometers

Antoine Weis (Invited speaker)

Physics Department, University of Fribourg, Fribourg, Switzerland

Abstract

Atomic magnetometers (AM)—also known as *optical magnetometers*—were introduced in the late 1950's. In the past 15 years AM R&D has received a new boost owing to the implementation of laser light for the AM operation. AM currently represent the most sensitive magnetometers and typically allow the detection of magnetic field changes in the one-digit femto-Tesla range (to note that this is 10 orders of magnitude less than the Earth magnetic field of $\approx 40 \mu\text{T}$!), some devices allowing even sub-fT detection sensitivity.

In my presentation I will briefly discuss the principle of atomic magnetometers which deploy optically-detected magnetic resonance in spin-polarized atomic vapors. The main part of my talk will focus on various AM-based applications in the field of biomedical imaging that have started to emerge around the world in the past decade. I will address in particular magneto-cardiography (MCG), magneto-encephalography (MEG), ultralow field MRI (ULF-MRI), and the very promising applications of magnetic nanoparticles (MNP). MNPs are already being deployed as contrast agents in MRI and for hyperthermia, but offer—in functionalized form—the possibility for targeted cancer treatment and biomedical imaging. For the latter application the technique of magnetic particle imaging (MPI) is particularly interesting, since it has already led to a commercial device that permits real-time angiographic imaging in small animals.

I will also address our own research work at UNIFR which focused on AM-based MCG in the past, and which is now centered on applying AMs both to MPI and to MRX (magnetorelaxation, another MNP detection technique) detection. To my knowledge, none of the mentioned methods has yet found its way into the daily clinical practice and it is very likely that atomic magnetometers will come to play an important role in future medical imaging devices.

Numerical simulation of X-ray grating interferometry imaging using Monte Carlo methods

S. Peter(1,2), M. K. Fix(3), P. Manser(3), M. Stampanoni(1,2)

(1) *Institute of Biomedical Engineering, ETH Zürich, Zürich, Switzerland*

(2) *Swiss Light Source, Paul Scherrer Institut, Villigen, Switzerland*

(3) *Division of Medical Radiation Physics and Department of Radiation Oncology, Inselspital, University Hospital and University of Bern, Bern, Switzerland*

Introduction

Hard X-ray grating interferometry (GI) is a recently established phase sensitive imaging technique with the advantage of simultaneously providing three complementary types of contrast: absorption, phase and dark-field contrast, which have been shown to have a wide range of possible applications in medical diagnostics and biomedical research. To address open questions about the details of the contrast formation process, such as the link between the measured signal and the physical properties of a sample, a numerical simulation framework using Monte Carlo methods (MC) has been developed.

Materials and Methods

For a realistic simulation of GI imaging, both particle-like and wave-like behavior of X-rays have to be considered. This was achieved by implementing two different approaches to include wave properties in MC. The first method was a combination approach where the X-rays are simulated as particles within MC for the source and sample part and then transformed into a wave and further propagated using wave-optics. The second approach was to include Huygens principle into the MC framework to account for interference.

Results

The framework was validated by comparison of simulated signals with experimental results and showed good agreement for both approaches. The results of the simulations performed with one of the models were used to describe the connection between the obtained signal and the physical structure of the sample in GI scattering signal. Potentially, this opens the possibility to a quantitative determination of unresolved sample features.

Conclusion

The good agreement between simulations and measurements validate the framework as a reliable simulation tool for GI. The results of the simulations were used for modeling the connection between the obtained signal and the physical structure of the sample which is of great importance for a quantitative evaluation and interpretation of the obtained image.

Task-based assessment of a the novel ADMIRE algorithm

Julien G Ott, Alexandre Ba, Damien Racine, Nick Ryckx, François O Bochud, Francis R Verdun

Institute of Radiation Physics, CHUV, Lausanne, Switzerland

Introduction

Over the last decade, Computed Tomography (CT) technology has improved and iterative reconstruction (IR) algorithms have led to drastic changes in image perception. In such a context, ensuring an adequate level of image quality while keeping patient exposure as low as reasonably achievable represents a new challenge that has to be addressed using clinically relevant tasks. The goal of this study is to report and investigate the performances of a new IR algorithm using a model observer that mimics human detection of low contrast targets.

Materials and Methods

A dedicated low contrast phantom (QRM, Moehrendorf, Germany) containing different targets (6 and 8 mm diameter; 10 and 20 HU at 120 kVp) was scanned at various CTDI_{vol} levels (1 to 15 mGy) on a Siemens SOMATOM Force CT. Images were reconstructed with a nominal slice thickness of 2.0 mm, using Advanced Modelled Iterative Reconstruction (ADMIRE) with 0 and 3 iterations. The images were assessed by three human observers, who performed a 4-alternative forced-choice detection experiment. Then, a Channelized Hotelling Observer (CHO) model with dense difference of Gaussian channels was applied on the same set of images. The comparison between the two was performed using their percentage of correct responses (PC) as a figure of merit.

Results

Our results indicated a strong agreement between human and model observer as well as a slight improvement in the low contrast detection when switching from 0 to 3 iterations. Indeed, for a 6 mm and 10 HU target at 3 mGy of CTDI and without any iteration performed, the PC for human reached $92.5 \pm 1.4\%$. CHO gave $91.5 \pm 4.4\%$. Under the same conditions with three iterations, the values reached $95.8 \pm 1.7\%$ for humans and $95.6 \pm 2.9\%$ for CHO.

Conclusion

This investigation showed the ability of the CHO model observer to reproduce human detection for a low contrast detection task, thus establishing its reliability for image quality assessment.

Good results in term of PC were also observed even in situations where the target was harder to detect (i.e. lower CTDI_{vol} and contrast level). All those elements suggest that patient dose could be further optimised and reduced thanks to the use of this new CT unit.

Texture analysis of CT perfusion maps - stability study

M. Nesteruk (1), R. Bundschuh (5), O. Riesterer (1), P. Veit-Haibach (2,3), G. Studer (1), S. Stieb (1), S. Glatz (1), H. Hemmatazad (1), G. Huber (4), M. Pruschy (1), M. Guckenberger (1), S. Lang (1)

(1) *Department of Radiation Oncology*

(2) *Department of Nuclear Medicine*

(3) *Department of Diagnostic and Interventional Radiology*

(4) *Department of Otorhinolaryngology*

University Hospital Zurich, University of Zurich, Switzerland

(5) *Department of Nuclear Medicine, University Hospital Bonn, Germany*

Introduction

The aim of this study was to identify a set of stable texture features computed in CT perfusion (CTP) maps in respect to CTP calculation parameters and image discretization.

Materials and Methods

Eleven patients with head and neck cancer and eleven patients with lung cancer who underwent diagnostic CT perfusion before a treatment were included in the study. A computer program for the calculation of texture features was developed based on definitions of the first-order statistical parameters, the Gray-Level Co-Occurrence Matrix, the Neighborhood Gray Tone Difference Matrix (NGTDM), the Gray Level Size Zone Matrix and the fractal dimension. 17 texture parameters were computed in the three perfusion maps: blood volume, blood flow and mean transit time. Texture parameters correlated with tumor volume were identified ($r > 0.7$). To investigate stability of texture parameters the intraclass correlation was calculated for potentially standardized (five Hounsfield Unit (HU) intervals and six discretization levels) and non-standardized factors (five different artery contouring and eleven noise thresholds). The texture feature was considered as stable if the intraclass correlation was higher than 0.7.

Results

Together 102 texture features were computed in the three perfusion maps and for the two tumor sites. Entropy, contrast from the NGTDM and fractal dimension were correlated with tumor volume. Potentially standardized factors introduced more variability into studied texture features than non-standardized. Summing up the results for the two patients groups, artery contouring and noise threshold affected the ranking of 15/102 and 27/102 parameters, respectively, whereas the discretization and HU intervals caused disagreement in 50/102 and 33/102 features, respectively. The first-order parameters, homogeneity and coarseness were found to be the most robust regarding CTP calculation parameters and image discretization.

Conclusion

Image discretization and HU intervals need to be standardized to build a reliable prediction model based on CTP texture analysis.

Intra- and interfraction motions assessed with Cone-Beam CT and fluoroscopy for lung SBRT

C. Castella (1), T. Breuneval (1), P. Tsoutsou (1,2)

(1) *Hôpital de Sion, Service de radio-oncologie*

(2) *Hôpital Neuchâtelois, Service de radiothérapie*

Introduction

The goal of this work was to evaluate the intra- and interfraction movements of patients undergoing lung stereotactic body radiation therapy (SBRT) treatments, using dedicated cone-beam computed tomography (CBCT) and fluoroscopy imaging protocols.

Materials and Methods

The first 13 patients treated in our center were investigated. Each patient received 60 Gy in 5 to 8 fractions, for a total of 76 fractions. Patients were immobilized with the ORFIT stereotactic positioning solution: a thermoplastic mask, a vacuum cushion, and a pneumatic pressure belt if deemed necessary. Three CBCT were acquired during each fraction (initial positioning, before beam-on and after beam-on) for assessing the quality of the immobilization. Additionally, orthogonal kV fluoroscopic images were analyzed in order to compare the online cranio-caudal movement with the one determined from the 4D planning CT. Finally, interfraction reproducibility was assessed by comparing the registration shifts recorded during the first fraction with those of the subsequent ones.

Results

Kolmogorov-Smirnov tests showed that the movement distributions along each axis were not significantly varying over time ($p=0.24$, 0.28 , and 0.98 for vertical, longitudinal, and lateral shifts), despite times between 1st and 2nd, and 1st and 3rd CBCT covering wide ranges depending on the patients ([7.2-20.9] VS [14.3-29.4] minutes, with respective means of 11.4 and 20.0 min). Moreover, 3D displacement vectors remained well below the 5 mm ITV-to-PTV margin used in our planning process ($p<0.01$). The amplitude of the lesion movement was precisely assessed by fluoroscopic imaging ($r=0.97$), further confirming the ITV shape. The interfraction reproducibility of the immobilization system was below 1 cm ($p=0.03$).

Conclusion

Combined with appropriate immobilization devices, this imaging protocol ensured that the 5 mm margin applied during planning was appropriate for treating the lesion correctly during the whole course of the treatment.

Modeling of a Robotic Treatment Table to improve the Control Performance

M. Stäuble(1), A. Jöhl(1,2), M. Schmid Daners(1), M. Meboldt(1), S. Klöck(2), M. Guckenberger(2),
S. Lang(2)

(1) *Product Development Group, Department of Mechanical and Process Engineering, ETH Zurich*

(2) *Department of Radiation Oncology, University Hospital Zurich*

Introduction

To reduce the planning target volume of lung tumors and, consequently, the volume of irradiated healthy tissue, respiratory tumor motion can be mitigated. The method considered in this work is the compensation of tumor motion by moving the patient with the treatment couch. Since the real treatment couch in question, the Perfect Pitch (Varian, Palo Alto, CA, USA), is part of the TrueBeam system and occupied in daily clinical use, a numerical model of the couch is of great use for simulating its dynamical behavior and to improve the control system of the couch without manipulating the controller of a medical device.

Materials and Methods

The numerical model of the Perfect Pitch was derived using Lagrange II and verified in this work. The equations of motion were implemented in MATLAB/Simulink. To gather data for estimating unknown parameters and validating the model, the TrueBeam developer mode was used. The couch's motion was generated by either using a sequence of control points stored in a predefined file or with a tumor motion phantom, which was tracked by Calypso (Varian, Palo Alto, CA, USA) using the iTools tracking mode. The accuracy of the numerical model was quantified using the root mean square (RMS) error. Furthermore, the performance of the iTools tracking mode was evaluated by measuring the error between the phantom and the treatment couch position.

Results

The average RMS error between the numerical model and the real treatment couch using the same input signal was 1.04 mm in longitudinal, 0.10 mm in lateral and 0.11 mm in vertical direction. The tracking error for the iTools tracking mode stayed below 2 mm for an input signal velocity of up to 20 mm/s in lateral and vertical direction.

Conclusion

This work shows that the treatment couch has great potential to compensate tumor motion due to respiration. However, a more sophisticated control strategy needs to be considered to meet the high tracking accuracy requirements also for fast respiratory tumor motion above 20 mm/s. The derived numerical model will be used to develop the control strategy.

A comparison of different respiratory motion management techniques

S. Ehrbar (1), R. Perrin (2), M. Peroni (2), K. Bernatowicz (2), T. Parkel (3), D. Ch. Weber (2), A. Lomax (2), I. Pytko (1), S. Klöck (1), M. Guckenberger (1), S. Lang (1)

(1) *University Hospital Zurich (USZ), Department of Radiation Oncology, Zürich*

(2) *Paul Scherrer Institut (PSI), Center for Proton Therapy, Villigen*

(3) *Centre Suisse d'Electronique et de Microtechnique (CSEM) S.A., Innovative Design, Landquart*

Introduction

Respiratory tumor motion enlarges the intra-fraction tumor position uncertainty. This increases the required treatment volume (PTV) and also the dose to organs at risk (OAR). Dosimetric performances of four motion-management techniques (MMT), dealing with intra-fractional respiratory tumor motion, were investigated: The internal target volume (ITV) concept with a PTV enclosing the whole tumor motion, the mid-ventilation (MidV) principle with probabilistic tumor margins, respiratory gating of the irradiation and treatment couch tracking with real-time compensation of the internal tumor motion.

Materials and Methods

The anthropomorphic, dynamic lung phantom LuCa (CSEM and PSI) was operated with 5 different respiration patterns with 10 to 20 mm internal tumor motion. 4DCT scans were taken and individual SBRT treatment plans were prepared, adapting the PTV according to the four MMT and five respiration patterns. A dose of 8x6 Gy was prescribed to the 65%-isodose line for each plan, as is done for rapidArc stereotactic treatment plans for early stage NSCLC at the USZ. The phantom was irradiated with each plan using the corresponding respiration pattern and MMT, together with static measurements. The respiratory tumor motion was monitored with Calypso (Varian) for gating and tracking treatments, and compensated with the PerfectPitch couch (Varian) for tracking. The dose in the tumor was measured with Gafchromic EBT2 (ISP) films. Changes in homogeneity indices (ΔH_{1-99}) and gamma agreement scores using 3%/3mm ($GS_{3\%/3mm}$) between the films and the planned dose distributions were evaluated. The film areas receiving more than the planned ITV minimum dose ($A_{>D_{min}}$) were calculated. OAR doses from the treatment plans were compared.

Results

Conclusion

All techniques achieved to cover the tumor with the prescribed 6 Gy. ITV and MidV showed lower gamma agreement scores and larger changes in inhomogeneity compared to tracking and gating. Tracking and gating showed comparable gamma agreement scores, and were able to reduce OAR dose in all cases, when compared to ITV concept.

Dosimetric Impact of Geometric Uncertainties in Navigated HDR-Brachytherapy for Liver Tumors

L. Witthauer (1), S. Weber (2), D. Terribilini (3), M.K. Fix (3)

(1) *Department of Physics, University of Basel*

(2) *ARTORG Center for Biomedical Engineering Research, University of Bern*

(3) *Division of Medical Radiation Physics and Department of Radiation Oncology, Inselspital, Bern University Hospital, and University of Bern, Switzerland*

Introduction

Navigated intra-operative interstitial high-dose-rate brachytherapy (HDR-IOBT) may have a therapeutic potential for certain hepatic malignancies as an alternative to other ablative interventions. The use of an instrument guidance system for HDR-IOBT that allows for accurate placement of the needles according to the pre-interventional calculated treatment plan would be beneficial for this application technique. Such a surgical navigation system has been previously developed for microwave ablation and open liver surgery. In this work, the dosimetric impact of the geometric uncertainties of such a navigation system for HDR-IOBT has been investigated.

Materials and Methods

Twelve different HDR treatments have been generated in Oncentra Masterplan (OTP V4.3.0.410) for a cylindrical water phantom containing a liver structure. These plans varied in the size of simulated spherical tumors between 1.5 and 8.4 cm and up to five needles. To account for the uncertainty of the navigation system, a C++ framework has been developed, which enabled the calculation of TG43 dose distributions, DVHs, and conformity numbers. The impact on these quantities was studied for randomly shifted needles either all together or one by one in the range of up to 5 mm. Additionally, needle rotations are studied.

Results

It was found that the reduction of the dose coverage for small (<5cm) tumors can be up to 50% for the needle shifts applied. For larger tumours, this reduction was less than 15%. Asymmetric needle settings yielded less stable dose distributions compared to symmetric settings, and fixing relative distances between the needles lead to a more robust dose distribution for different needle settings.

Conclusion

It was shown that a navigation system for HDR-IOBT with an accuracy of 5 mm is feasible for tumors with a diameter larger than 5 cm. Furthermore, the calculation showed that the usage of a template would be beneficial for the dose conformity.

Feasibility study of using a radiofrequency tracking system for intra-fractional monitoring during radiosurgery

I. Pytko, A. Stüssi, S. Lang, S. Klöck, M. Guckenberger

University Hospital Zurich, Department of Radiation Oncology

Introduction

Modern linear accelerators perform stereotactic radiosurgery (SRS) and radiotherapy (SRT) treatments with sub-millimeter accuracy in dose delivery, as well as image guided patient setup. However, intra-fractional patient motion is a source of uncertainty in these treatments. The feasibility of using the Calypso (Varian, USA) radiofrequency tracking system for intra-fractional motion monitoring during cranial SRS treatments was evaluated.

Materials and Methods

Studies were performed using the Calypso system with wireless surface transponders. For the measurements, the Alderson head phantom was used. Additionally, 3 volunteers and 2 patients were evaluated. The transponder was positioned with a sticky tape behind the ear of the phantom and accuracy of couch shifts and couch rotations were evaluated with respect to the PerfectPitch couch (Varian, USA). On volunteers 3 different transponder locations were tested. Maximal motion of the whole brain patient (10x3Gy) as well as of the SRT patient (6x5Gy) planned with 2 couch rotations was recorded. As the position of the Calypso tracking array is defined in the treatment room, additional feasibility of using the system was retrospectively evaluated from CT scans of 40 intracranial tumor volumes.

Results

Calypso detected couch shifts with a 3D accuracy of 0.14 (± 0.31) mm and the rotational isocenter run-out was 0.22 (± 0.22) mm. The measured jitter was 0.2 (± 0.1) mm which led to overall accuracy of 0.33 (± 0.34) mm. Both patients showed maximal motion of 0.8 mm in the longitudinal direction. Out of the 40 intracranial tumor volumes, 36 would be feasible to treat with the system.

Conclusion

Intra-fractional motion can be monitored using the Calypso system with an accuracy of less than 1mm necessary for the SRS treatments. The possibility of using the Calypso surface transponder for the stereotactic treatments was shown on two pilot patients.

A dosimetric comparison of MERT and mixed beam therapy for selected head and neck tumors

A. Joosten, S. Müller, D. Henzen, W. Volken, D. Frei, D.M. Aebbersold, P. Manser, M.K. Fix

Division of Medical Radiation Physics and Department of Radiation Oncology, Inselspital, Bern University Hospital, and University of Bern, Switzerland

Introduction

The aim of this study is to perform a dosimetric comparison between Modulated Electron Radiation Therapy (MERT) and mixed electron-photon beam therapy with variable number of photon beams in terms of tumor coverage, sparing of nearby healthy tissues and reduction of low dose bath for selected head and neck tumors.

Materials and Methods

Three head and neck cases were selected for MERT and mixed beam planning. For each case, several non-isocentric electron fields were setup at short SSD (~70cm) and up to four different energies were considered for both the MERT and the electron component of the mixed beam plans. For the mixed beam plans, plans were created with 2, 4, 6 and 8 isocentric photon fields respectively which were optimized on top of the electron plan contributing half the dose to the PTV. The dose homogeneity indexes (HI) in the PTV, the mean and max doses in OAR as well as the low dose bath were investigated.

Results

Mixed beam plans with at least 4 photon fields result in a better PTV coverage (HI>96%) than MERT plans. Compared to MERT, mixed beam plans with 4 photon fields substantially reduce the mean and max dose to OAR in the close vicinity of the PTV. Mixed beam plans with 6 or 8 photon fields do neither improve the PTV dose coverage nor reduce the dose to nearby OAR but result in larger doses to remote OAR and an increase of the low dose bath.

Conclusion

Compared to MERT, mixed beam plans improve dose homogeneity to the PTV while sparing more efficiently OAR nearby the PTV. The results suggest that the lower the number of photon beams are selected, the lower the low dose bath is for mixed beam plans. This work was supported by KFS-3279-08-2013.

Knowledge based planning model assessment for breast VMAT planning

A.Fogliata(1), C.Bourgier(2), F.DeRose(1), P.Fenoglietto(2), F.Lobefalo(1), P. Mancosu(1), S.Tomatis(1), M.Scorsetti(1), L.Cozzi(1)

(1) *Humanitas Research Hospital, Radiotherapy and Radiosurgery Dept, Rozzano-Milan, Italy*

(2) *ICM-Val d'Aurelle, Radiotherapy Dept, Montpellier, France*

Introduction

To evaluate the performance of a model-based optimisation process for volumetric modulated arc therapy applied to whole breast irradiation.

Materials and Methods

A set of 150 volumetric modulated arc therapy dose plans were selected to train a model for the prediction of dose-volume constraints. The model was built to manage whole breast irradiation with simultaneous integrated boost. The dosimetric validation was done on different groups of patients from two institutes for single (35 cases) and bilateral breast (10 cases).

Results

Quantitative improvements (statistically significant for many of the analysed dose-volume parameters) were observed between the model-based and the reference plans. Of 320 dose-volume objectives assessed for plan evaluation for unilateral breast, 12% the reference plans failed to respect the constraints while the model-based plans succeeded. Only in 1% of the cases the reference plans passed the criteria while the model-based failed. In 10% of the cases both groups of plans failed and in the remaining cases both passed the tests. For the bilateral breast analysis, the model-based plans resulted superior or equivalent to the reference in 95% of the cases.

Conclusion

The data suggests that the dose-volume constraint personalisation can be efficiently and effectively automated for VMAT breast planning, by the use of the new engine and could encourage its application to clinical practice.

A clinical distance measure for evaluating radiotherapy treatment plan quality difference with Pareto fronts

K. Petersson(1), A. Kyroudi(1), J. Bourhis(2), F. Bochud(1), and R. Moeckli(1).

(1) *Institute of Radiation Physics (IRA), Lausanne University Hospital, Lausanne, Switzerland*

(2) *Department of Radiation Oncology, Lausanne University Hospital, Lausanne, Switzerland*

Introduction

Pareto front evaluation has proven useful for evaluating radiotherapy treatment plans. However, it is difficult to quantify Pareto fronts, distances between fronts, or between a front and a given plan. It is also difficult to conclude if any difference in distance is of clinical significance. Hence, the purpose of our study was to develop a mathematical metric that can be used for plan comparison and that mitigates these limitations of Pareto front studies.

Materials and Methods

The clinical distance is composed of a Euclidian distance and a clinical scaling factor, which scales the distance between different evaluation parameters in a plan. The scaling factor can thereby add clinical meaning to an otherwise purely mathematical distance. To test the clinical distance, two-dimensional (2D) Pareto fronts (PTV coverage vs. rectum dose) were created for five cases of prostate cancer. Sub-optimal treatment plans were also created in order to test various distances from a plan on each front. The clinical distances between Pareto optimal and sub-optimal plans were compared with clinically evaluated plan quality (clinical grading analysis, CGA) in order to verify that the plan quality difference perceived by radiation oncologists and medical physicists is in agreement with the measure.

Results

The clinical distance increases as the perceived plan quality difference increases. At a 2D distance of around 0.30 (0.28-0.35), the physicist and radiation oncologists agree that there is a significant difference in plan quality between the Pareto optimal and the sub-optimal plans (i.e. the clinical resolution). This occurs at a lower threshold value of 0.23 if the measure takes into account variations in all evaluation parameters (nD).

Conclusion

The clinical distance can be used to determine if the difference between a front and a given plan (or between different fronts) corresponds to a clinical significant plan quality difference. The measure can take into account variation in all evaluation parameters, i.e. it can quantify plan quality difference in 2D to nD Pareto front studies. The clinical distance removes many of the known limitations that suppress the use of Pareto front evaluation for comparing radiotherapy treatment plans.

Monte Carlo Based Analysis of Dose Rate Distributions in Volumetric Modulated Arc Therapy

P.-H. Mackeprang, W. Volken, D. Terribilini, D. Frauchiger, K. Zaugg, D.M. Aebbersold, M.K. Fix, P. Manser

Division of Medical Radiation Physics and Department of Radiation Oncology, Inselspital Bern University Hospital, and University of Bern, Switzerland

Introduction

Data on the variation of dose rate in Volumetric Modulated Arc Therapy (VMAT) is not known in current treatment planning systems. In VMAT, both machine dose rate and collimation change dynamically and hence affect the dose rate for every individual voxel during dose delivery within one fraction. In this work, a tool was developed to evaluate dose rate distributions using Monte Carlo techniques.

Materials and Methods

VMAT treatment plans are split into arc sectors between consecutive DICOM control points. By calculating dose distributions in units of cGy/Monitor Unit for each of these sectors of planned constant dose rate and multiplying with machine dose rates, dose rate distributions are obtained for every voxel at every time point during a treatment fraction. Histograms of dose rates in the planning target volumes were generated for a head and neck case. Further, the standard deviations of dose rates over the course of the fraction were analyzed for each voxel.

Results

For the selected case, PTV dose rates ranged from 0 cGy/min to 462.48 cGy/min with a mean per arc of 34.57 cGy/min to 86.65 cGy/min. Standard deviations of dose rates calculated per voxel over one arc ranged from 0.15 cGy/min to 167.71 cGy/min.

Conclusion

Spatio-temporal distributions of dose rate can now be assessed for each voxel in a calculation volume at any time during a fraction.

PHILIPS

Pinnacle³

Treatment Planning



**Flexible, intuitive
planning environment**

A comparison of 6 planning RT techniques for breast treatments

M.Zeverino (1), N. Ruiz Lopez (1), M. Marguet (1), W. Jeanneret Sozzi (2), J. Bourhis (2), F. Bochud (1), R. Moeckli (1)

(1) CHUV, Institute of Radiation Physics

(2) CHUV, Department of Radiation Oncology

Introduction

To provide a comparison of 6 different treatment planning strategies, adopted for breast conserving-adjuvant RT, on the dose to the PTV and OARs.

Materials and Methods

22 patients CT data sets were retrospectively used for planning comparison. Patients were split in two groups of 6 left- and 5 right-sided cases (G1 and G2) according to the different dose prescription (50 Gy in 25 fractions and 42.4 Gy in 16 fractions for G1 and G2, respectively). The 6 techniques involved were: Field in Field (FiF), 2 Fields static-IMRT (sIMRT-2ff), 4 Fields static-IMRT (sIMRT-4FF), VMAT, Helical Tomotherapy (HT) and Tomo Direct (TD). Dose limits applied to PTV and OARs were taken from the RTOG protocol n.1005. Treatments plans were optimized to reduce dose to Ipsilateral Lung (IL), Contralateral Breast (CB) and, for left-sided cases, Heart (H) while maintaining an acceptable PTV coverage and homogeneity.

Results

The highest mean value $V_{95\%}=98.8\%/99.2\%$ (G1/G2) was observed for TD and it was statistically significant with respect to all others techniques except to VMAT. Similar results were obtained for $D_{98\%}$. The lowest mean $V_{105\%}=0.2\%/0.1\%$ (G1/G2) was found for HT resulting statistically significant if compared to all other techniques except FIF/VMAT in G1 /G2, respectively. Mean $D_{2\%}$ was also found lowest for HT (52.1Gy/43.1Gy in G1/G2) resulting statistically significant with respect to all other techniques except versus TD in G2. For IL mean $V_5(\text{Gy})$, $V_{10}(\text{Gy})$ and dose mean were lowest for TD in both groups (20.1%/19.1%, 14.2%/13% and 5.8%/4.9% in G1/G2, respectively) being statistically significant versus all other techniques in G1. The lowest values of mean $V_{20}(\text{Gy})=7.0\%/7.9\%$ were observed for HT in both groups. CB dose maximum was found as lowest in G1 for TD (290.9cGy) and for FiF in G2 (252,6cGy) both resulting statistically significant versus all other techniques except for FiF in G1 and TD in G2 confirming a substantial equivalence for the two techniques. Minor absolute dose differences were observed for H.

Conclusion

6 different techniques were employed to design an optimal plan for conserving breast-adjuvant RT fulfilling the dose limit criteria provided by RTOG 1005 protocol. TD provided superior target coverage maintaining a level of homogeneity similar to HT which achieved the highest value. IL dose was minimized with TD while dose to CB was lowest using both FiF and TD techniques.

A clinical protocol for Simultaneous Integrated Boost for proton treatment

MF Belosi, R Malyapa (MD), A Bolsi, AJ Lomax, DC Weber (MD)

Paul Scherrer Institut, Center for Proton Therapy (5232 Villigen

Introduction

Simultaneous Integrated Boost (SIB) has already been exploited in conventional radiation therapy with photons for several treatment sites. At the Paul Scherrer Institute (PSI, Villigen CH) we have designed a planning study to define the SIB protocol for Head and Neck (H&N) patients using PBS proton therapy. Particular attention was focused on finding optimization parameters and a normalization procedure to reduce over-dosage in the fall off area of the boost without compromising the coverage.

Materials and Methods

Four patients, originally treated at PSI with a conventional schedule for malignant neoplasms of the parotid gland (2 patients) and nasopharyngeal lateral wall (2 patients), were selected for this study. All have been re-planned using a SIB regime of 1.8Gy fractions (up to 54Gy) to PTV1 and 2.36Gy (up to 70.8Gy) to PTV2 for a total of 30 fractions. Dose constraints to the OARs were kept constant from sequential to SIB approach. All plans were designed on the PSIPlan Treatment Planning System using IMPT (Intensity Modulated Proton Therapy) with 3 non-coplanar fields. The 100% dose corresponded to the dose to PTV1, while the dose to PTV2 was optimized prescribing a boosting factor of 131% , which corresponds to the ratio of the two different prescribed dose levels (i.e. 54GyRBE and 70.8 GyRBE). The obtained IMPT trial was finally normalized to PTV1-(PTV2+3mm). A 3 mm margin to PTV2 was added in order to account for the dose gradient in close proximity to the boosted volume and obtain a more homogeneous dose distribution within the PTV1-PTV2 ring.

Results

The quality and conformity of the SIB plans was observed to be dependent on the volume ratio of PTV2/PTV1 (calculated only for the cranio-caudal extension where both are defined). For the analyzed patients, this ranged from 34.7% to 89.3%. The SIB approach resulted in a lower mean dose to the ring area (55.5+0.6 GyRBE on average for SIB; 59.8+3.5 GyRBE on average for sequential), whilst preserving 95% dose coverage to the PTV1. In one case (with the highest PTV2/PTV1 volume ratio of 89.3%), no difference was observed in the two treatment approaches. A similar sparing of OARs was obtained with SIB as for the original plans.

Conclusion

Planning H&N patients with SIB optimization resulted in dose distributions which guaranteed the PTV2 and PTV1 coverage and conformity whilst keeping dose to OARs within tolerance. Therefore this approach can be transferred to the clinical operation and has already been applied to a first patient.

Improving lateral penumbra using contour scanned proton therapy

Gabriel Meier (1,2), Dominic Leiser (1,3), Rico Besson (1), Alexandre Mayor (1), Sairos Safai (1), Damien Charles Weber (1,3), Antony John Lomax (1,2)

(1) *Paul Scherrer Institut, Center for Proton Therapy,*

(2) *ETH Zurich*

(3) *Inselspital, University of Bern*

Introduction

Pencil beam scanned (PBS) proton therapy allows for reduced integral dose compared to conventional photon therapy. So far, clinical fields are made up of several thousand Bragg peaks (BP's) distributed on a rectilinear grid. However, by placing BP's directly on the surface of the target volume, we believe that higher dose conformation may be possible than using rectilinear distributions. It was the aim of this work to investigate the planning and delivery aspects of this contour scanning approach for skull-base tumors.

Materials and Methods

With contour scanning, BP's are placed along geometrical contours orthogonal to the field direction. These are then repeatedly shrunk to create a set of concentric closed paths along which BPs can be placed. Using this approach, plans have been created for several chordoma cases and qualitative dose measurements using CCD and film have been performed to validate the deliverability of the technique on Gantry 2 at PSI.

Results

A reduction of dose to critical organs positioned laterally to the beam (e.g. brain stem, chiasm) of the order of ten to twenty percent could be achieved over all cases, at the cost of a slightly reduced dose homogeneity (D5/D95) in the PTV of 3.4 (\pm 0.2)%. The predicted effects are also visible in dose measurements performed in solid water for a cylindrical target, as well as for irregularly shaped targets in an anthropomorphic head phantom. Dose reductions of up to 20% in organs at risk (OARs) were measured, corresponding to a 2mm shift of the 50% isodose as well as a 15% reduction of the penumbra.

Conclusion

Contour scanning has the potential to reduce the dose to OARs in the vicinity of the target volume while allowing for equal target coverage, albeit with slightly reduced dose homogeneity. Predicted dose differences have been measured in simple geometries as well as an anthropomorphic head phantom. The approach can further be improved by optimizing the spacing between concentric contours thus allowing for sharper penumbrae

TransitQA - Concept of transit dosimetry for Tomotherapy treatments

O. Pisaturo(1), F. Miéville(1), P-A. Tercier(1), A.S. Allal(1)

(1) HFR - Hôpital fribourgeois, Service de Radio-Oncologie

Introduction

Interfraction discrepancies can occur along the treatment of a patient and result in significant differences with the initial treatment plan. These variations can be imputable to changes in the patient morphology and positioning, as well as delivery errors that can occur during a specific fraction. In this context, verification is a particularly essential step in the treatment procedure. In this study, an efficient method for Tomotherapy transit dosimetry using the on-board detector (OBD) has been developed.

Materials and Methods

The attenuated normalized detector sinogram acquired by the OBD during treatment is compared with the processed TPS sinogram (plan side), corrected for patient transmission. The transmission profiles are obtained using the pre-treatment megavoltage computed tomography images (MVCT). The difference in the energy spectra between the imaging and treatment beam is corrected by an exponent consisting in the ratio of the mass attenuation coefficients. A way to take into account patient position corrections due to image registration has also been derived. The whole method has been validated with plans calculated in the Tomotherapy Cheese phantom in homogeneous and heterogeneous configurations.

Results

The ratio of the mass attenuation coefficients has been calculated for different materials and appears not to depend on the atomic number. This shows that the model can be applied to heterogeneous materials in the beam path, such as a patient. This is also confirmed by our results in the Cheese phantom in every tested configuration. The method applied over the whole treatment of a patient show significant differences between fractions.

Conclusion

A comprehensive procedure for transit dosimetry has been developed for Tomotherapy treatments. It does not need any external device and does not disturb the patient workflow. Moreover, the patient does not receive any extra dose in the process.

A general model of stray dose calculation of static and intensity-modulated photon radiation beams

P.Hauri(1,2), Roger A. Hälgl(2), J.Besserer(2), and Uwe Schneider(1,2)

(1) *Faculty of Science, University of Zurich, Zurich, Switzerland*

(2) *Radiotherapy Hirslanden, Hirslanden Medical Center, Aarau, Switzerland*

Introduction

There is an increasing number of cancer survivors who are at risk for late effects caused by ionizing radiation such as induction of second tumors. Hence, the determination of out-of-field dose for any particular treatment plan in a patient's anatomy is of great concern. The purpose of this study was to analytically model the stray dose according to its three major components.

Materials and Methods

For patient scatter, a mechanistic model and for collimator scatter and head leakage, an empirical model was developed for a 6MV nominal beam energy of two Varian linear accelerator types. The parameters of the model were trained using chamber measurements of total absorbed dose in simple geometries. Whole-body dose measurements of thermoluminescent dosimeter in an anthropomorphic phantom for static and intensity modulated treatment plans were compared to the model's calculated 3D out-of-field dose distribution.

Results

The absolute average deviation of four different plans between the calculated and the measured stray dose was 11% with a maximum discrepancy below 44%. Computation time of 36'000 dose points for one field was around 30 s. By fusing the calculated out-of-field with the treatment planned dose the whole-body dose distribution can be viewed in the treatment planning system.

Conclusion

The results suggest that the model is accurate, fast, and can be used for a wide range of treatment modalities to calculate the whole-body 3D out-of-field dose for clinical analysis. An advantage of the mechanistic patient scatter model is that for similar energy spectra it can be used independently of treatment machine or beam orientation.

A novel approach to the reference dosimetry of proton pencil beams based on dose-area product

C. Gomà(1), B. Hofstetter-Boillat(2), S. Safai(1), S. Vörös(2)

(1) *Centre for Proton Therapy, Paul Scherrer Institut*

(2) *Federal Institute of Metrology METAS*

Introduction

This work presents a novel approach to the reference dosimetry of proton pencil beams based on dose-area product (DAP). DAP is the integral of the absorbed dose to water (D_w) over the plane perpendicular to the beam direction. The determination of DAP of a narrow proton pencil beam with a large detector is compared to the standard determination of D_w at the center of a broad field with a small detector.

Materials and Methods

First, we calibrated a PTW Bragg Peak chamber (BPC) in terms of DAP in the METAS ^{60}Co beam. Second, we determined the beam quality correction factor (k_Q) of the BPC experimentally. Finally, we determined the DAP of a proton pencil beam following IAEA TRS-398 formalism and we compared it to the standard determination of D_w at the center of a broad proton field with a PTW Markus chamber.

Results

The BPC was successfully calibrated in terms of DAP in a ^{60}Co beam. The uncertainty of the calibration coefficient was slightly larger than in the standard case, due to the uncertainty of the sensitive volume radius. The ratio of k_Q factors of the BPC and Markus chamber was found to be 1.009(5). The DAP and standard approaches were found to agree within one standard deviation.

Conclusion

This work shows that the reference dosimetry of proton pencil beams based on DAP is equivalent to the standard approach based on D_w . Its only drawback is a slightly larger uncertainty of the IC calibration coefficient. This novel approach could also be used in the reference dosimetry of small photon beams.

Comparison of various dosimeters at high dose-rate

M. Jaccard (1), K. Petersson (1), C. Bailat (1), T. Buchillier(1), J. Bourhis(2), R. Moeckli(1) and F. Bochud(1)

(1) *Institut de Radiophysique (IRA), Lausanne University Hospital, Lausanne, Switzerland*

(2) *Department of Radiation Oncology, Lausanne University Hospital, Lausanne, Switzerland*

Introduction

Preclinical animal studies have shown that irradiation by a pulsed electron beam with high dose-rate allows for tumour control while sparing normal tissues. Dosimetry of high dose-rate pulsed beam is challenging because of dose-rate dependence and saturation effects. We discuss some of the recent dosimetric results obtained with a prototype linac capable of such dose-rates.

Materials and Methods

In this study, the dose-rate was varied between a few Gy per minute (conventional) and 1000 Gy per second ("Flash"), by modifying the repetition frequency of the pulses and their characteristics, i.e. height and width. This modulation of the beam made possible the investigation of dosimeters behaviour over a large dose-rate range. Measurements and comparisons were performed with a parallel-plate ionization chamber (the Advanced Markus), EBT3 Gafchromic films, LiF thermoluminescent dosimeter (TLD) and methyl viologen (chemical dosimeter). All of which were traceable to national primary standards.

Results

We obtained excellent consistency between all the dosimeters at conventional dose-rate which confirmed their proper calibration. Further results showed that films, TLD and viologen dose measurements were in good agreement over the entire dose range and no sign of dose-rate dependence was found. In contrast, the ionization chamber displayed saturation which is shown to depend, at first order, only on the dose per pulse.

Conclusion

Our dosimetric evaluation shows that TLD, Gafchromic films and viologen do not saturate at high dose-rates and their response is not affected by the pulsed structure of the beam. The saturation of the Advanced Markus at high-dose rate can be modelled and depends primarily on the dose per pulse.

3d printed dose compensation body to remove dose artifacts of a HDR Brachytherapy surface applicator of the vertical type.

K. Buchauer, L. Plasswilm, H. Schiefer

Klinik für Radio-Onkologie, Kantonsspital St.Gallen

Introduction

Unflattened surface HDR Brachytherapy applicators commonly suffer from dose fall off on the side of the dose distribution. Recent research documented that in addition to missing dose at the side of the applicator vertical type HDR Brachytherapy surface applicators are subject to underdose in the middle of the treatment region due to a possibly tilted source in addition to self absorption in the longitudinal direction of the source. This artifact is clinically relevant because tumor cells in the middle of the treated area can end up irradiated insufficiently. In this work we present a surface-dose compensation body generated with a 3D printer that specifically addresses the dose irregularities of a vertical type HDR Brachytherapy surface applicator.

Materials and Methods

Previously investigated surface dose irregularities were used as a starting point to define the thickness profile of the compensation element. A 40 mm applicator was used as prototype applicator for the modification. The source position is 1.5 cm from applicator tip. The depth of evaluation is 0.5 cm solid water material. The nominal diameter of the dose distribution therefore equals 53.3 mm when a 50% isodose level as size definition is considered. A consumer grade 3D printer "UP! 3D, Beijing TierTime Technology Co. Ltd." was used to print out a negative form with ABS plastic. Lippowitz type low temperature melting metal was used to mold the positive form of the compensation body of a prototype flattening element for a 40 mm vertical type surface applicator.

Results

The generated compensation element is of toroidal shape with a maximum thickness of 1.5 mm in surface direction. The output reduction as consequence of the flattening element occurred to be 25%. The diameter of 80% nominal dose increased from 35.2 cm with the unflattened applicator to 48.9 mm with the flattening element in place. The central underdosed region is compensated with the flattening element.

Conclusion

The presented prototype of a dose compensation body can remove the dose artefacts of a vertical type HDR Brachytherapy surface applicator including the clinical relevant underdosed central region.

Research Activities at the Bern Medical Cyclotron

M.Auger¹, S.Braccini¹, T.S.Carzaniga¹, A. Ereditato¹, K. Nesteruk¹, P. Scampoli^{1,2}

(1) *Albert Einstein Center for Fundamental Physics (AEC), Laboratory for High Energy Physics (LHEP), University of Bern, Sidlerstrasse 5, CH-3012 Bern, Switzerland*

(2) *Department of Physics, University of Napoli Federico II, Complesso Universitario di Monte S. Angelo, I-80126, Napoli, Italy*

Introduction

The Bern cyclotron laboratory is located at the Bern University Hospital (Inselspital). It is based on a 18 MeV proton cyclotron equipped with a specifically conceived 6m long research beam transfer line (BTL), terminated in a separate bunker. This is a very peculiar feature for a hospital-based facility. Thanks to this particular configuration, in parallel with routine clinical production of PET radioisotopes, various research activities can be carried on. They include developments in beam monitoring devices, new radioisotopes and radiation protection.

Materials and Methods

An accurate assessment of beam intensity, position and shape is crucial for an optimal production of radionuclides and for research activities using charged particle beams. A novel non-destructive beam monitor detector (UniBEaM) based on optical fibres was developed and its commercialization is on-going. For the study of new radioisotopes for diagnostics and therapy, new irradiation methods are studied including a compact mini beam line. The accurate radiation protection is both a safety and a research tool. In particular, it allows performing studies of air contamination.

Results

The UniBEaM beam monitoring detector was used to study the proton beam produced by the Bern cyclotron. Precise profiles were obtained with currents ranging from a few μA down to the pA range. On this basis, the transverse beam emittance of the cyclotron was measured. Sc-43 is proposed as a novel PET radioisotope and the production cross section for the reaction $^{43}\text{Ca}(p,n)^{43}\text{Sc}$ was measured. A study of the radioactivity produced by protons extracted into air was performed using both theoretical calculations and experimental measurements.

Conclusion

The Bern cyclotron laboratory is fully operational since 2013. It allows daily PET radiotracer production together with multi-disciplinary research activities. The most recent results on novel beam monitoring detectors, new radioisotopes and radiation protection will be presented.

Changing from ITV to MidV concept - Do we have to increase the prescribed dose?

A. Tartas (1,2), S. Ehrbar (2), L. S. Stark (2), M. Guckenberger (2), S. Klöck (2), S. Lang (2)

(1) *University of Warsaw, Faculty of Physics, Warsaw, Poland*

(2) *University Hospital Zurich, Department of Radiation Oncology, Zürich*

Introduction

The internal target volume concept (ITV) is a commonly used concept for stereotactic body radiation therapy (SBRT) of lung cancer. Recently, the mid-ventilation (MidV) principle which is a probabilistic margin approach to ensure that 90% of the patients receive 95% of the dose was introduced. This approach leads to reduced margins and a better sparing of the healthy tissue. This work investigated, whether the prescribed dose needs to be increased, changing from the ITV to the MidV concept to ensure the same amount of GTV dose coverage.

Materials and Methods

Twenty lung cancer patients were analyzed in this study. For all patients four-dimensional (4D) CT images were taken and treatment plans for ITV and MidV concepts were prepared. The full tumor excursion was delineated as ITV and planning target volume (PTV) margins of 5 mm were added. For the MidV concept, margins according to the van-Herk formula were added to the GTV in the MidV phase. VMAT treatments plans were calculated with a dose of 3x13.5 Gy prescribed to the 65% isodose around the PTV for both techniques. Time-resolved 4D dose calculations linking breathing motion and dynamic delivery were performed, where the dose to the GTV was added up in MIM Maestro (MIM Software Inc., USA) using deformable registrations. For both concepts the summed up doses to the GTV were compared to the planned doses in the GTV or ITV.

Results

The mean 3D tumor motion was 12.9 mm (range: 4.9-27.3 mm). For the ITV concept the planned mean dose to the ITV was 60.2 (± 0.4) Gy (mean (\pm standard deviation)) and 60.5 (± 0.4) Gy to the GTV using the MIDV concept. The time resolved 4D calculations for the ITV concept lead to an increased GTV mean dose of 0.5 (± 0.5) Gy compared to the mean ITV dose. For the MidV concept the mean dose to the GTV was reduced by 1.8 (± 0.7) Gy compared to the 3D calculation, and this difference was increasing with increasing tumor motion. The mean dose to the lung with tumor was 18% ($\pm 8\%$) less for the MidV concept compared to ITV concept.

Conclusion

It is recommended to increase the dose per fraction from 13.5 Gy to 14 Gy when changing from the ITV concept to the MidV concept in order to ensure that the mean dose in the GTV is the same.

Proton radiography for the clinical commissioning of the new Gantry2 head support at PSI

L. Placidi, S. König, R. van der Meer, F. Gagnon-Moisan, A. J . Lomax, D. C. Weber, A. Bolsi

Paul Scherrer Institut, Center for Proton Therapy

Introduction

The treatment couches for Gantry2 will support new head pieces for head and neck treatments, the BoS Headframe™ (Qfix, Avondale, Pennsylvania, USA). Thanks to their geometry and composition (a sandwich of very thin carbon layers and light foam) they will increase the flexibility of planning, as they should only minimally disturb proton beams passing through it. We describe here the main part of the commissioning process, which was the measurement of their Water Equivalent Range (WER) and homogeneity.

Materials and Methods

Mono-energetic scanned proton layers (12x20cm²) of 129 MeV up to 145 MeV were delivered through the head support, with the proton dose on exit being measured using a scintillating screen/CCD camera device approach. In order to perform measurements at end of proton range, 10cms (equal to 11.67cm of WER) of plexiglass (plus 0.7cm WER from a PVC slab embedded in the CCD camera before the scintillating foil) were positioned between the head support and the active area of the CCD camera. A reference set of measurements were first performed without the head support with 1 MeV discrete energy steps. The measurements were then repeated through three different positions (head, neck and shoulder) of the head support. In two critical areas of the headframe (shoulder and head&neck) a second set of measurements were performed with an energy step of 0.2 MeV for energies between 133-139 MeV, to increase the measurement accuracy. For each acquisition, a 2D map of the maximum values among all the layers was generated, from which the WER of the head support in the different positions could be calculated by subtracting the measurements with and without the frame. WER homogeneity was calculated as the standard deviation of sub-regions of the 2D difference maximum value maps.

Results

Head support WER's of between 2.4mm and 7.2mm were measured with an accuracy of 1.0mm for the 1.0 MeV energy steps and 0.5mm for the 0.2 MeV steps, depending on the areas examined. The obtained homogeneity for the head, neck and shoulder was 0.36mm, 0.99mm and 0.40mm respectively.

Conclusion

The described method for the evaluation of the BoS Headframe™ homogeneity and WER thickness was accurate, fast and reproducible. The results on the thickness and homogeneity of the headframe show that it can be used in clinical operation.

Eye tracking analysis of treatment plan evaluation in radiotherapy

A. Kyroudi (1), K. Petersson (1), M. Ozsahin (2), J. Bourhis (2), F. Bochud (1), R. Moeckli (1)

(1) *Institute of Radiation Physics (IRA), Lausanne University Hospital, Lausanne, Switzerland*

(2) *Department of Radiation Oncology, Lausanne University Hospital, Lausanne, Switzerland*

Introduction

Treatment plan evaluation is a clinical decision-making problem that involves visual search and analysis in a contextually rich environment, including delineated structures and isodose lines superposed on CT data. In an approach similar to what has been done in radiology since the 1970's, we studied the feasibility of using eye-tracking techniques to enhance the understanding of how decision makers interact with the given visual information during treatment plan evaluation.

Materials and Methods

Single transverse slice dose distributions of ten prostate cancer treatment plans were presented to eight decision makers (radiation oncologists and medical physicists). Their eye-fixation positions were recorded with an EyeLink1000 remote eye-tracker and determined through pupil and corneal reflection created by infrared illumination.

Results

The main results included the plan evaluation time, number and duration of fixations in the areas of interest, and saccades per decision maker and per plan. Our results show great variability among decision makers, with radiation oncologists performing longer first fixations to the rectum.

Conclusion

This study allowed us to present the type of results which can be acquired with the eye-tracking method. Based on our results we could suggest different visual behaviors related to the background and the expertise of the decision makers.

StereoPHAN™, an end-to end phantom for SBRT

F. Hasenbalg, T. Buchsbaum, C. Erckes, K. Haller and P. Pемler

Klinik für Radioonkologie, Stadtspital Triemli Zürich

Introduction

Patient specific quality assurance (QA) is especially important in stereotactic body radiotherapy (SBRT) where doses up to 15 Gy per fraction are delivered usually in 3 to 10 sessions. A new commercially available anthropomorphic head phantom, StereoPHANTM, from Sun Nuclear Corporation has been tested as an end-to-end solution for quality assurance purposes.

Materials and Methods

The stereotactic phantom, StereoPHANTM, has been used as a test patient undergoing the whole treatment chain. It was scanned using his several inserts (film, ion chamber, and CT localization). The image registration among the several inserts has been checked.

SBRT plans were then realized and verified on it using both radiochromic film dosimetry (GafChromic™ EBT3 and EBT-XD from Ashland , Inc.) and ionization chamber measurements at the center of the phantom (3D PinPoint chamber from PTW Freiburg GmbH).

Results

Image registration among the different inserts of the phantom and to its built -in markers were at the sub-millimeter level (< 1mm). The SBRT plan verifications gave gamma passing rates of approximately 95%, for a gamma criterion of 2% dose difference / 2 mm distance-to-agreement. Ionization chamber measurements gave a good agreement (< 1%) with TPS calculations.

Conclusion

StereoPHANTM proved to be a well designed and useful as an end-to-end verification phantom for SBRT treatments.

A Novel Approach of Customized Shielding in Superficial and Orthovoltage Radiotherapy

M. Baumgartl(1), A. Dietschy(2), K.S. Bertapelle(2), Dr. S. Hemm-Ode(2), A. Pfäfflin(3), Dr. G. Kohler(1)

(1) *University Hospital Basel, Clinic of Radiotherapy and Radiation Oncology*

(2) *University of Applied Sciences Northwestern Switzerland, School of Life Sciences, Institute for Medical and Analytical Technologies*

(3) *Bildungszentrum Gesundheit Basel-Stadt*

Introduction

Standard applicators in kilovoltage x-ray beam therapy do not always fit to the shape of target volumes. Therefore, customized shielding to spare healthy tissue is nowadays mainly based on in-house leaded foils attached to the applicators. However, the production of customized shields could be time consuming and provides not always a promising result. An adequate, fast and reproducible approach of shielding was developed to treat the target volume in the low and medium energy (kV) range for rectangular applicators.

Materials and Methods

Two different shielding systems were developed. In our department in Basel (USB) 60% of all in-house shields were carried out with straight-edged lead elements [1]. They are coated with a plastic foil to prevent skin contact to the toxic lead and to the produced secondary electrons. For an easy attachment of the shielding to the applicator magnets were used. Those were glued to a 1cm broad PMMA frame with an identical size of a standard applicator which attach to magnets elongating along the edge of the applicator. The magnets and the frame do not interfere with the radiation field. The other side of the frame is covered with hook-and-loop fastener (Velcro). Lead elements were covered as well on the one side with a hook-and-loop fastener and on the other side with a plastic foil, respectively. Straight-lined shields can be adjusted within seconds to shape the target volumes. A second approach allows to shield more sophisticated target volumes with LEGO elements covered with overlapping lead elements and plastic foil attached to a LEGO frame instead of a PMMA frame. All archived target volumes were rebuilt and the customized area analyzed.

Results

All used straight-lined shields from our database could be exactly reproduced contouring 100% of the target volume using the hook-and-loop fastener system. In contrast the LEGO system is more adaptable to shape sophisticated target volumes but is limited to the rectangular nature of the LEGO elements leading to an additional irradiation of healthy tissue. In average 12.4% of this healthy structure beyond the target volume would be irradiated more.

Conclusion

Shielding healthy tissue in superficial and orthovoltage radiotherapy using the reusable hook-and-loop fastener and/or the LEGO system promises a fast exchange of shields for different target volumes with a reproducible accuracy. Furthermore the magnetic frame system allows to irradiate multiple target volumes in a row with the same rectangular applicator.

Reference

[1] Bertapelle K S and Dietschy A, Felddausblockungen für die Röntgentherapie, Bachelorprojekt, University Hospital Basel, Herbst 2014

Evaluation of Machine Performance Check

M. Zamburlini(1), I. Pytko(1), A. Stüssi(1), T. Rudolf(1), S. Klöck(1), S. Lang(1)

(1) *Klinik für Radio-Onkologie, UniversitätsSpital Zürich*

Introduction

As linear accelerators become more sophisticated, quality assurance (QA) becomes increasingly complex and time consuming. Varian (Varian Medical System, USA) introduced with True beam version 2.0 a new QA tool called Machine Performance Check (MPC), thanks to which the stability of beam output and machine geometry can be verified in a simple and time wise fashion.

Materials and Methods

The primary goal of this study was to investigate the ability of MPC to detect deviations from the baseline in the Linac output, MLC position, and gantry and jaws position. To prove the MPC sensitivity to detect these discrepancies, we miscalibrated the photon and electron output by 2%, introduced a 0.5 mm misalignment in the MLC position, a 1 mm misalignment in the jaw position and an error in gantry position. We compared then the MPC detected discrepancy to the introduced error. The second goal was to understand how MPC compares with our daily QA performed at the machine and which current QA procedures it could substitute.

Results

MPC was able to detect the introduced error with good accuracy. For example a 2% deviation in the beam output produced a 2.3 % deviation in the MPC beam output (for all tested beam energies). MPC was less satisfactory for what concerns the amount of QA procedures it could substitute. At the moment it is not possible to perform wedge and energy measurements, and it is not possible to analyze beam profiles. In this first version it is, in addition, not possible to customize the checks. These limitations mean that it cannot fully replace our QA procedures and therefore can be used only as an add-on QA procedure effectively increasing the QA time.

Conclusion

MPC has great potential to monitor the Linac performance and detect deviations from the baseline values, however at the moment it does not help in reducing the QA time.

Variability of PET image noise as function of acquisition and reconstruction parameters and its usefulness for quantifying tumor hypoxia

R. Kueng (1), P. Manser (2), M. Fix (2), H. Keller (1)

(1) Princess Margaret Cancer Centre, RMP ; (2) Inselspital Bern, AMS

Introduction

The values in a PET image which represent activity concentrations of a radioactive tracer are influenced by a large number of parameters that characterize the conditions of the patient, the image acquisition and image reconstruction. On top of this, variability exists between different PET scanners and PET operators which is of great concern for multi-center clinical trials. For example, one metric described in the literature to characterize hypoxia in tumors (hypoxic fraction) is based on the noise characteristics in a background structure (e.g. a muscle). Therefore, in this work, noise characteristics in PET images have been investigated for various parameters describing image acquisition and image reconstruction.

Materials and Methods

Different phantoms with homogeneous activity distributions were scanned using various acquisition parameters and reconstructed with various reconstruction parameters. Images from on-site GE Discovery 610 PET/CT scanner and other PET scanners were analyzed and compared with respect to quantitative noise behavior. Local noise metrics, which are the basis of quantifying hypoxic fraction, as well as global noise measures in terms of noise power spectra were computed. In addition to variability due to different reconstruction parameters, spatial variability of activity distribution and its noise metrics were investigated. Patient data from clinical trials were mapped onto phantom scans to explore the impact of the scanner's intrinsic noise variability on quantitative clinical analysis.

Results

While local mean values were relatively stable with respect to varying reconstruction parameters, local noise metrics were varying up to an order of magnitude for different reconstructions. As for the acquisition parameters (absolute background concentration and acquisition time), noise metrics were in agreement with the familiar Poisson statistics. Also, the degree of slice overlap was a crucial aspect, since noise varied strongly along axial direction for a single bed position scan. For all scanners, the local noise was larger in the center of a phantom (up to 50%) compared to the outer regions. Additionally, the on-site GE scanner demonstrated a radial variability of 5-10% for local mean values. Mapping of patient data from a trial showed that a PET scanner's spatial noise variability had a significant influence on the value of the hypoxic fraction (absolute threshold value varying up to 15%).

Conclusion

We showed that a hypoxic fraction metric based on noise characteristics requires careful consideration of the various dependencies in order to justify its quantitative validity. This work may result in recommendations for harmonizing PET imaging for multi-institutional clinical trials.

MC Simulation of Electron Transport in Homogeneous Magnetic Fields: Dosimetric Effects for MeV Electron Beams

S. Höfel (1,3), D. Frei (2), P. Manser (2), M.K. Fix (2)

(1) *Klinik für Strahlentherapie/Radiologische Gemeinschaftspraxis, Gesundheitsverbund Landkreis Konstanz, Konstanz, Germany*

(2) *Division of Medical Radiation Physics and Department of Radiation Oncology, Inselspital, Bern University Hospital, and University of Bern, Switzerland*

(3) *Klinik und Poliklinik für RadioOnkologie und Strahlentherapie, University Hospital Klinikum rechts der Isar, Technische Universität München, Munich, Germany (current address)*

Introduction

Recently, the realization of MRI-LINAC systems has experienced considerable progress. Moreover, the idea of shaping the dose distribution especially from electron beams by applying strong magnetic fields has been reported in the literature. In this work we analyzed the dosimetric impacts of transverse or longitudinal oriented homogeneous magnetic fields on the dose distribution from MeV electron beams for academic situations.

Materials and Methods

Mono-energetic electron pencil beams with perpendicular incidence on a homogeneous cubic water phantom were simulated using the Monte Carlo (MC) code GEANT4. Dose distributions for various combinations of magnetic field strength B (0, 0.5, 1, 2, 3, 5 and 7 T), initial electron energy E (1, 2, 4, 6, 10, 15, 20 and 25 MeV) and magnetic field orientation (transverse or longitudinal) were obtained. PDDs and broad beam dose distributions were then calculated by lateral dose integration and lateral superposition, respectively. Changes in the dosimetric characteristics of the PDDs and in the lateral beam profiles were analyzed. In case of the transverse magnetic field orientation, trajectories of hypothetically unscattered electrons were calculated for various magnetic field strengths by numerically solving the electrons relativistic equation of motion.

Results

In case of a transverse magnetic field the central axis PDDs of broad electron beams change strongly compared to the field-free situation: e.g. for $B = 7$ T and $E = 25$ MeV the practical range R_p decreases by a factor of 10, the peak dose increases by a factor of 11 and the depth of dose maximum decreases by a factor of 19. The peak to surface dose ratio exhibits a remarkable maximum at approximately $B = 1$ T for energies greater than 2 MeV. For longitudinal magnetic fields the lateral dose fall-off is steepened, e.g. for $B = 7$ T and $E = 10$ MeV the penumbra 80%-20% decreases by a factor of 4.3. The calculated trajectories of unscattered electrons reflect the high dose region of the corresponding pencil beam dose distributions.

Conclusion

A transverse magnetic field of 0.5 T already affects the central axis PDDs of broad beams considerably. Strong transverse magnetic fields confine the dose to shallow depths. Hence, the therapeutic volume shrinks. Peak dose enhancement occurs due to spiralling electrons. Longitudinal magnetic fields affect the dose distribution where no lateral electron equilibrium is provided, i.e. mainly at the beam edges, thus leading to penumbra reduction. The calculated electron trajectories are useful for understanding and interpretation of the dose effects observed.

On the RapidArc commissioning tests by Ling et al. 2008: the IOSI experience with old and new tests.

G. Nicolini, A. Clivio, E. Vanetti (1)

(1) *Ente Ospedaliero Cantonale, Medical Physics, Bellinzona (Switzerland)*

Introduction

At the introduction of RapidArc (RA) technique, the paper by Ling et al. 2008 has constituted a reference, proposing RA machine quality assurance (QA) tests. Since 2008, many centers overall the world have been able to run similar QA tests, thanks to free availability of RT plan dicom files from the Varian website. Recently, part of these tests were redrawn with new suggestions; tests identified as T2 ("variation of dose rate (DR) and gantry speed(GS)") and T3 ("variation of MLC Speed (MLCS)") were better tune respect delivery parameters.

Materials and Methods

Our experience with the first RA QA tests version on three different Varian linacs (Clinac iX, Unique, TrueBeam) is summarized; data were collected through portal vision (PV) images, since installation date with a monthly periodicity, for respectively 80, 21, and 44 entries. After reviewing the characteristics, new plans have been acquired and analyzed for all the 6MV beams, energy suggested for the tests. Original tests were extended to 10MV, 6FFF and 10FFF beams for TrueBeam. For FFF beams two plans versions were investigated, with a different maximum DR: 800 and 1400 for 6FFF, and 600 and 2400 MU/min for 10FFF; for the highest DR the PV was moved out of isocenter position (SDD=150cm) to avoid saturation.

Results

First version of the test T2 and T3, have presented during time differences respect reference value greater than 2% (always lower 3%), for Clinac iX and Unique, while TrueBeam data were always <2%. The first T2 band presents a systematical higher value respect the others, behavior common also to other machines and centers, we were in contact with, explainable with some weakness in the test itself. New T2 and T3 tests, showed an agreement well below 2% for all the 3 linacs. The renormalization of values respect the open field, was performed both manually and automatically, as ROI ratio and as ROI on image ratio. The second approach guarantees an higher degree of reproducibility of results.

Conclusion

New tests demonstrated to be more robust and we have moved as routinely checks, in our QA monthly program. A study on possibility of other test versions, able to support the user in an eventually troubleshooting investigation is in its delineation phase. Although out of the scope, a comparison with dose calculation in TPS would be of interest.

The Current Status of the Implementation of Clinical Audits in Switzerland

M. Gasser(1), R. Treier(1), Ph. R. Trueb(1)

(1) Swiss Federal Office of Public Health FOPH, Division of Radiological Protection

Introduction

In a period of 15 years (1998-2013) the exposure of the Swiss population by medical X-rays in diagnostic radiology increased by 40% [1,2]. While in the past much effort has been made to optimize radiological procedures, the aspect of justification of the examination itself has not been considered sufficiently. Clinical audits constitute a proven method of identifying and minimising unjustified examinations and treatments with ionising radiation as well as optimising processes and resources. Within the framework of a peer review system a team of physicians, medical physicists and radiographers review the work processes of their colleagues with regard to good clinical practice. According to the European level directive 2013/59 EURATOM, all member states must carry out clinical audits in accordance with national procedures by 2018. Although not a member of EURATOM, Switzerland has also decided to implement its guidelines.

Methods and Results

The Swiss Federal Office of Public Health (FOPH) has established an interdisciplinary expert group consisting of representatives of medical professional societies in order to implement clinical audits in Switzerland. This group has developed the conception of the project and a legal text which is now included into the revised Swiss Radiological Protection Ordinance. For the ongoing pilot phase three working groups were set up in the fields of radiology, radiation oncology and nuclear medicine. They have established checklists and requirements for quality manuals. In the field of radiology the focus of the pilot audits is on procedures and processes of CT examinations, in nuclear medicine on procedures and processes of PET-CT examinations, and in radiation oncology on the whole patient pathway. Furthermore, the auditors have been trained in auditing techniques. Currently the audit contents are evaluated by European experts from different fields. The first pilot audits are scheduled for this autumn.

Conclusion

Clinical audits prove to be an essential tool to increase quality in patient care significantly by identifying and eliminating unjustified radiological processes and optimizing justified radiological processes.

For the implementation of clinical audits in Switzerland all relevant stakeholders were involved in different processes already in an early stage. International standards were assessed and, where needed, adapted to the local situation. It was observed that a restriction of the focus on selective topics (according to a graded approach) allows an efficient use of resources. With this nationally adopted approach a substantial progress in the implementation was possible.

References

[1] Nation-wide Survey on Radiation Doses in Diagnostic and Interventional Radiology in Switzerland in 1998, 1998, IRA

[2] Nation-wide Survey on Radiation Doses in Diagnostic and Interventional Radiology in Switzerland in 2013, 2013, IRA (preliminary report)

An adequate Quality Assurance technique for superficial hyperthermia equipment

G. vanStam(1), D. Marder(1), M. Capstick(2), O. Timm(1), G. Lutters(1)

(1) *RadioOnkologieZentrum KSA-KSB, Kantonsspital Aarau, Switzerland*

(1) *Foundation for Research on Information Technologies in Society (IT'IS), Zürich, Switzerland*

Introduction

Radiotherapy and Hyperthermia (RT+HT) appears to be a successful combination for superficially located breast cancer. The heating pattern of the applicator should regularly be tested to guarantee the quality of the HT treatment. Integrating of regular QA measurements in the work flow requires a fast and cost efficient technique to measure the Specific Absorption Rate (SAR). Therefore, a measurement setup with an agar phantom and an infrared camera is presented.

In this study the setup with the agar phantom on two commercially available- and one new hyperthermia applicator; the 915 MHz 14 cm round Archimedean 8 Spiral Array (BSD SA-812), the 434 MHz 14.8 x 14.3 cm Contact Flexible Micro-strip (CFMA-2H), and the 434 MHz 7.5 x 7.5 cm Cavity Backed Slot (IT'IS CBSA) is tested.

Materials and Methods

A vertically splittable (muscle equivalent) flat agar phantom (25 x 25 x 8 cm) and a removable 1 cm thick agar top layer were developed to determine both the Effective Field Size (EFS; i.e. 50% isoSAR) at 1cm depth and the Effective Heating Depth (EHD; i.e. distance between 100% at 1 cm depth and 50% SAR). The applicator with a thin water bolus was positioned on top of the phantom. An infrared camera (Optris-PI 160x120) was positioned at a fixed (55 cm) distance from the phantom surface, to measure the heating pattern (is proportional to the SAR) at the surface before and after a 2 min power pulse. The phantom must be split vertically (EHD) or the 1 cm layer removed (EFS) before the picture of the heating pattern can be taken.

Results

The EFS and EHD of the three applicators can be determined. The measurement accuracy of the measured EFS and EHD, compared to the values of the suppliers and found in published papers, is better than 10% and 30% respectively.

Conclusion

A fast and cost efficient technique to perform QA measurements for superficial applicators was developed. This enables integration of regular measurements in the work flow, which is essential to ensure HT treatment quality. The agar phantom has to be renewed after a few months.

A method for pre-treatment verification of hyperthermia treatment plans

D.Marder*, N.Brändli, G.vanStam and G.Lutters (1)

(1) *RadioOnkologieZentrum KSA-KSB, Kantonsspital Aarau, Switzerland*

Introduction

The BSD-2000/3D system (BSD Medical Cooperation, Salt Lake City, USA) is used to treat deep seated tumors with hyperthermia (to temperatures of 41-43°C) in combination with radiotherapy. Treatment planning for this system is done with the software SigmaHyperplan (Dr. Sennewald Medizintechnik GmbH, Munich, Germany). In this study a method and first results for pre-treatment verification of clinical patient treatment plans using a 3D SAR scanning phantom developed at the Kantonsspital Aarau are presented.

Materials and Methods

Treatment plans for individual patients were generated with SigmaHyperplan and applied to a scanned saline phantom model. The result is a set of data for the specific absorption rate (SAR) distribution.

The measurement data is obtained with a saline phantom consisting of a tube with elliptical cross section. The tube is inserted into the BSD-2000/3D Sigma60 and a probe inside is moved in 3 spatial dimensions. The probe, a commercial isotropic SAR sensor, is scanned in 2 cm steps for a distance of 20 cm in horizontal and vertical directions and relative SAR values are recorded.

Planned and measured data in the central plane of the applicator are compared for the location of the focus to assess the transferability of treatment plans to the treatment machine.

Results

The location of the focus maximum can be determined from the graphs and compared to the location of the maximum from the simulation. For the investigated plans an agreement between simulation and measurement was found with deviations of the focal area between 0 and 2 cm.

Conclusion

Good agreement for the investigated patient plans was found between simulation and measurement. With an automated measurement system higher resolutions and 2D or 3D comparisons would be possible. The method described allows the transferability of a patient treatment plan to the treatment machine to be verified, however it does not check the correct heating of the patient.

Comparison of Image Quality and Radiation Exposure between Dental Volume Tomography DVT and Conventional CT by Using a Novel Skull - DLP Phantom

C. Sommer(1), I. Oezden(2), G. Lutters (2), A. Cornelius (3) S. Scheidegger (1,2)

(1) *ZHAW School of Engineering*

(2) *Kantonsspital Aarau, Institute of Radiation Oncology*

(3) *Institute for Radiology*

Introduction

With the introduction of Dental or Digital Volume Tomography (DVT), an ongoing discussion about radiation exposure compared to more conventional CT scans with maxilla-facial or dento-facial indications started. Therefore, we developed a novel skull phantom for simultaneous evaluation of image quality and radiation exposure.

Materials and Methods

The skull phantom consists on a PMMA cylinder with an elliptical cross section with an effective diameter of approx. 16 cm containing a central and 4 peripheral wholes for dose length product (DLP) chambers (similar to the IEC standard phantom), vertebral bodies and elements for measuring image quality parameters and an extension with a cats skull. The skull is embedded in a water-equivalent resin (Translux D150, Axson Technologies). Image quality and DLP have been measured simultaneously by scanning the phantom using a DVT (Carestream CS 9300C, tube voltage 90 kV) and a CT (Toshiba Aquilion One ViSION, tube voltage 100 kV) with the corresponding protocols. To evaluate the influence of scatter, measurements with a 10cm - and a 30cm chamber (PTW Unidos) have been compared.

Results

The measurements of the DLP and CTDI are for both modalities in the same region (DLP: 44-46 mGy*cm, CTDI: 4-6 mGy). Although the SNR values for CBCT is significantly lower (12, CT: 30), the CBCT image was preferred by the radiologist due to the better high-contrast resolution. The estimate for the effective dose is for both modalities 0.09 mSv.

Conclusion

Compared to earlier measurements, the difference of radiation exposure between CT and DVT seems to become smaller with the use of newer CT units. Based on the qualitative rating of representation of bone structures, DVT seems to be a valuable alternative to scans of the maxilla-facial region with more conventional CT.

Comparative patient dosimetric estimates for different radiological facilities when performing maxillofacial examinations

Marta Sans-Merce (1,2), Jérôme Damet (1), Minerva Becker (2)

(1) *Institut de radiophysique, CHUV, Suisse*

(2) *Hôpitaux Universitaires de Genève, Suisse*

Introduction

Maxillofacial radiologic examinations often result in irradiation of the thyroid gland, parotid glands and lens due to primary exposure or radiation scatter. Organ exposure depends on imaging modalities and protocols. The purpose of this investigation was to evaluate radiation doses to the above-mentioned organs for CT, cone beam CT (CBCT) and panoramic radiographs (orthopantomography, OPT).

Materials and Methods

The absorbed dose was measured on the surface of a head phantom with thermoluminescence dosimeters. The phantom was imaged with CT, CBCT and OPT using standardized protocols employed in clinical routine. The areas examined included the paranasal sinuses, the entire head and the mandible depending on the protocol used. Dose measurements were performed individually for each modality and each protocol.

Results

Doses to the thyroid gland when located outside the area of interest were lowest for all modalities (range: 0.01-1.22mGy; measurement uncertainty: 10% at $k=2$). Depending on the examination protocol, doses to the eye lens (due to primary beam or scattered radiation) showed wide variability (range: 0.02 - 26.22mGy). The parotid glands were the only organs systematically placed in the primary beam for all modalities and protocols. Values ranged from 1.40-29.11mGy with the highest values for CT examinations. For OPT, doses to the parotid glands were strongly inhomogeneous due to its operating mode.

Conclusion

CT was the most irradiating modality. The mean doses to the parotid glands were similar for CBCT and OPT, while doses to organs in the scattered field were systematically higher for CBCT than OPT.

Verification and validation of a cylindrical 3D water scanner

T. Götzfried, A. von Deschwanden (1)

(1) *Radiation Oncology, Cantonal Hospital of Lucerne*

Introduction

Nowadays, water scanning systems are extremely accurate and precise. Nevertheless, some basic quality assurance should be adopted to ensure that a scanning system comprising a water tank, positioning system, ionization chambers and an electrometer, is capable of performing satisfactorily.

Materials and Methods

In addition to checks on detectors, electrometers and software, we focus on the mechanical operation of Sun Nuclear's 3D SCANNER. The automatic-setup procedure provides means to automatically level the tank, zero the detector position to water surface, align the scanner's coordinate system to the linac system, and correct motor hysteresis. The cylindrical water tank uses a scanning mechanism consisting of three motorized drives (ring, diameter, and vertical). Mechanical alignment as well as movement accuracy and reproducibility are assessed by using a caliper, a precision dial gauge and a plumb line.

Results

Leveling of the tank or ring, respectively, results in 0.2mm/m. The vertical position of the filled tank is stable and deviations can be specified to be $< 0.5\text{mm}$ (over 3 hours). Positioning accuracy in horizontal and vertical direction is $< 0.2\text{mm}$, for ring rotation $< 0.2^\circ$. Reproducibility of motion is checked by moving the probe using a single motorized drive. All positions confirm the accuracy of motion to be within 0.05mm.

Conclusion

Even though manufacturers of scanning systems offer annual preventive maintenance services, the user should still verify the integrity and accuracy of the water scanning system.

List of participants

| Lastname | Firstname | 21st | 22nd | Dinner | Location |
|-------------------|------------|------|------|--------|-------------------|
| Alonso | Sara | 1 | 1 | | Aarau |
| Baumgartl | Michael | 1 | 1 | | Basel |
| Belosi | Francesca | 1 | 1 | | Villigen |
| Binder | Jörg | 1 | 1 | 1 | Aarau |
| Braccini | Saverio | 1 | | | Bern |
| Bubula-Rehm | Edyta | 1 | 1 | 1 | Basel |
| Buchauer | Konrad | | | | St. Gallen |
| Buchillier | Thierry | 1 | 1 | | Lausanne |
| Buchsbaum | Thomas | 1 | | | Zürich |
| Bulling | Shelley | 1 | 1 | | Genève |
| Burkard | Walter | | 1 | | |
| Carzaniga | Tommaso | | | | |
| Castella | Cyril | 1 | 1 | 1 | Sion |
| Chatelain | Cécile | | 1 | | Bienne |
| De Vecchi | Cecilia | 1 | 1 | | Villigen |
| Di Domenicantonio | Giulia | 1 | 1 | 1 | Genève |
| Di Pasquale | Giovanna | 1 | 1 | 1 | Genève |
| Domingues Ginja | Tania | 1 | 1 | | Fribourg |
| Ehrbar | Stefanie | 1 | 1 | | Zürich |
| Emert | Frank | 1 | 1 | 1 | Villigen |
| Ernst | Marina | 1 | 1 | | Zürich |
| Fachouri | Nanta | 1 | 1 | | Villigen |
| Favre | Pascal | 1 | 1 | | Bienne |
| Fix | Michael | 1 | 1 | | Bern |
| Fogliata | Antonella | 1 | 1 | | Milano |
| Gasser | Michael | 1 | 1 | | Bern |
| Gnesin | Silvano | 1 | 1 | 1 | Lausanne |
| Goma Estadella | Carles | 1 | 1 | | Villigen |
| Götzfried | Thomas | 1 | | | Luzern |
| Guibert | Geoffroy | 1 | 1 | | La Chaux-de-Fonds |
| Haller | Käthy | | 1 | | Zürich |
| Hasenbalg | Federico | | 1 | | Zürich |
| Hauri | Pascal | | | | Zürich |
| Hirschi | Lukas | 1 | 1 | 1 | Bergen, Norway |
| Höfel | Sebastian | | | | |
| Icken | Niels | 1 | | | Aarau |
| Ionescu | Victor | 1 | 1 | | Marly |
| Ionescu | Florica | 1 | 1 | | Marly |
| Ith | Michael | 1 | 1 | | Bern |
| Jaccard | Maud | 1 | 1 | 1 | Lausanne |
| Joosten | Andreas | 1 | 1 | 1 | Bern |
| Jungo | Philippe | 1 | 1 | | Fribourg |
| Käser | Yvonne | 1 | 1 | | Uetikon |
| Kottler | Christian | 1 | 1 | | Bern-Wabern |
| Koutsouvelis | Nikolaos | 1 | 1 | 1 | Genève |
| Kueng | Reto | | | | |
| Kyroudi | Archonteia | | | | Lausanne |
| Lang | Stephanie | 1 | 1 | | Zürich |
| Leick | Mauricio | | 1 | 1 | Chêne-Bougeries |
| Lima | Thiago | 1 | 1 | 1 | Aarau |
| Lomax | Tony | | | | Villigen |
| Mackeprang | Paul-Henry | 1 | 1 | | Bern |
| Madry-Gevecke | Britta | 1 | | | Münsterlingen |
| Manser | Peter | 1 | 1 | 1 | Bern |
| Marder | Dietmar | | 1 | | Aarau |
| Markert | Barbara | 1 | | | Münsterlingen |
| Miéville | Frédéric | 1 | 1 | 1 | Fribourg |
| Miltchev | Vesselin | 1 | 1 | 1 | Allschwil |
| Moeckli | Raphaël | 1 | 1 | | Lausanne |

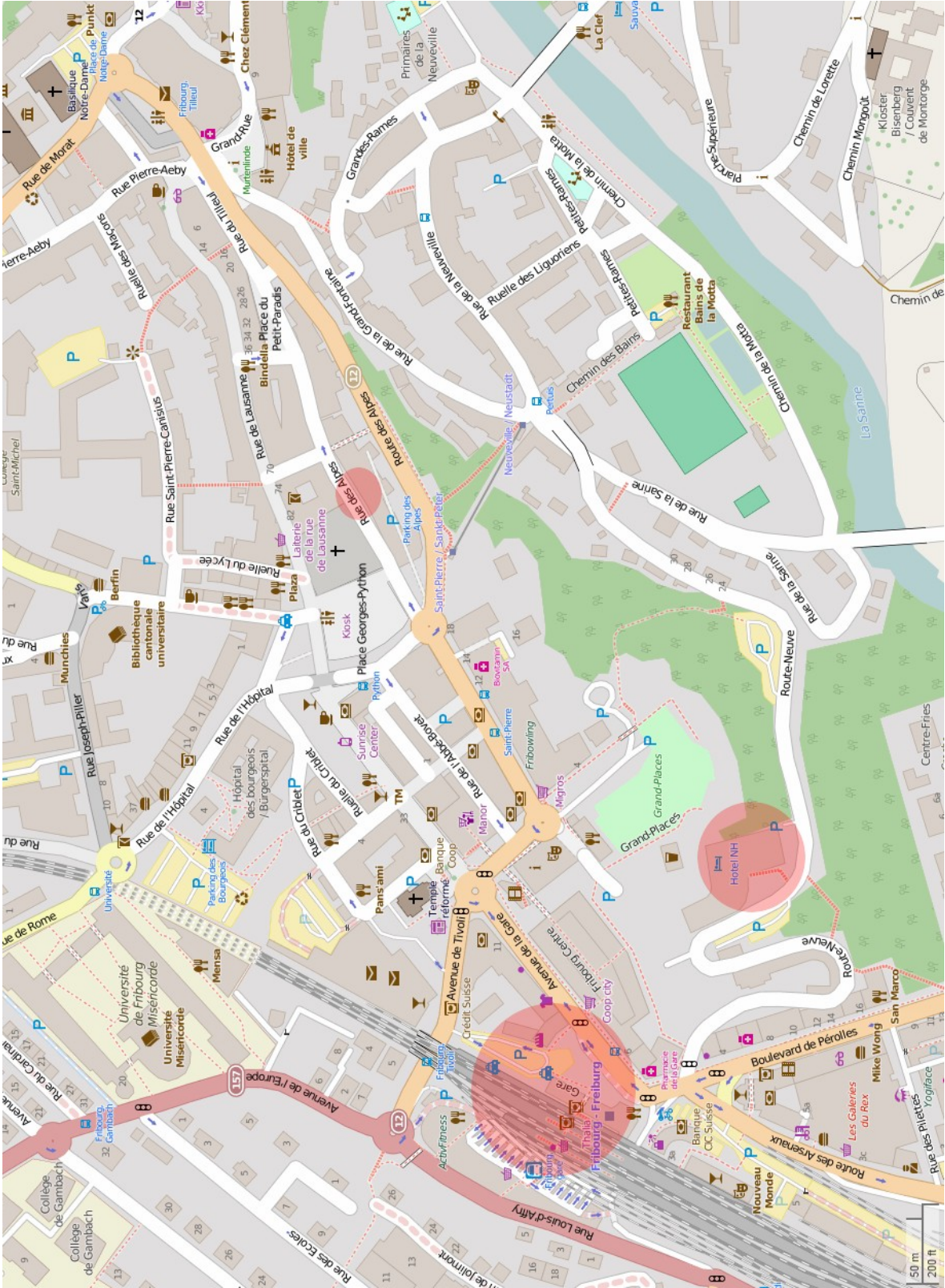
| | | | | | |
|---------------------|--------------|---|---|---|-------------------|
| Müller | Silvan | 1 | 1 | 1 | Bern |
| Najar | Alain | | 1 | | |
| Nesteruk | Marta | 1 | 1 | | Zürich |
| Neuenschwander | Hans | | 1 | | Bern |
| Nicolini | Giorgia | 1 | 1 | | Bellinzona |
| Nowak | Marie | 1 | 1 | 1 | Lausanne |
| Oezden | Ismail | 1 | 1 | | Aarau |
| Ott | Julien | 1 | 1 | 1 | Lausanne |
| Pemler | Peter | 1 | | | Zürich |
| Peretti | Frédérique | 1 | 1 | 1 | |
| Peter | Silvia | 1 | 1 | | Villigen |
| Peters | Samuel | 1 | 1 | | St. Gallen |
| Petersson | Kristoffer | 1 | 1 | | Lausanne |
| Pierre-Justin | Henri | 1 | 1 | 1 | |
| Pisaturo | Olivier | 1 | 1 | 1 | Fribourg |
| Placidi | Lorenzo | 1 | 1 | | Villigen |
| Presilla | Stefano | 1 | 1 | | Bellinzona |
| Pytko | Izabela | 1 | | | Zürich |
| Racine | Damien | 1 | 1 | | Lausanne |
| Rakotomiaramananana | Barinjaka | | 1 | | Bern-Wabern |
| Ryckx | Nick | 1 | 1 | 1 | Lausanne |
| Safai | Sairos | 1 | 1 | 1 | Villigen |
| Saltybaeva | Natalia | 1 | | | Zürich |
| Sans Merce | Marta | 1 | | | Lausanne |
| Schmidhalter | Daniel | 1 | 1 | | Bern |
| Schnekenburger | Bruno | 1 | 1 | 1 | Winterthur |
| Schopfer | Mathieu | 1 | 1 | | Lausanne |
| Schöpflin | Robert | 1 | | | St. Gallen |
| Seiler | Regina | 1 | 1 | 1 | Luzern |
| Sheib | Stefan | 1 | 1 | 1 | Baden |
| Silveira | Joao | 1 | 1 | | |
| Sommer | Olaf | | 1 | | Winterthur |
| Sommer | Christian | 1 | 1 | | Winterthur |
| Soumova | Andrea | 1 | 1 | | Hünenberg |
| Stäuble | Markus | 1 | 1 | | Zürich |
| Suner | Joel | 1 | 1 | 1 | Feldkirchen |
| Tamburella | Claire | 1 | 1 | | La Chaux-de-Fonds |
| Taranenko | Valery | 1 | 1 | 1 | Lausanne |
| Tartas | Adrianna | | | | Zürich |
| Tercier | Pierre-Alain | 1 | 1 | 1 | Fribourg |
| Thengumpallil | Sheeba | 1 | | | Chêne-Bougeries |
| Treier | Reto | 1 | 1 | | Bern |
| Trueb | Philipp | 1 | | | Bern |
| Van Stam | Gerard | 1 | 1 | | Aarau |
| Vetterli | Daniel | 1 | 1 | 1 | Biel |
| Vlachopoulou | Vasiliki | 1 | 1 | | Chur |
| Vugts | Lia | 1 | 1 | | Aarau |
| Weber | Patrick | 1 | | | La Chaux-de-Fonds |
| Weis | Antoine | 1 | | | |
| Wirz | Marcel | 1 | 1 | | Bern-Wabern |
| Witthausen | Lilian | 1 | 1 | 1 | Basel |
| Zamburlini | Mariangela | | 1 | | Zürich |
| Zeaverino | Michele | 1 | 1 | 1 | Lausanne |
| Zucchetti | Paolo | | 1 | | Luzern |

Situation MAP

The big red circle is the train station

The middle one is the NH-Hotels

The small circle is the Restaurant « Aigle Noir »

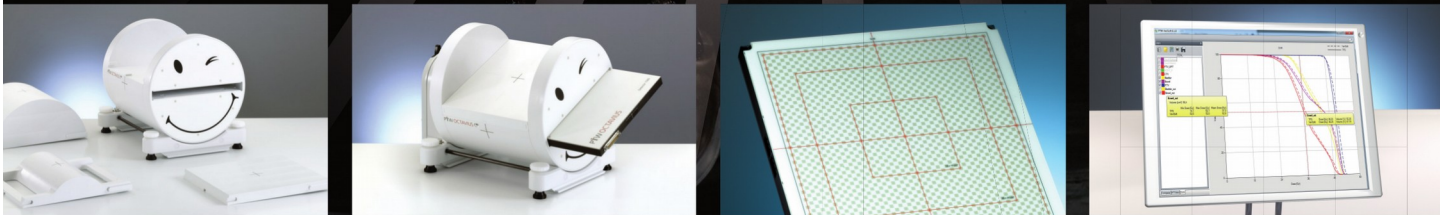


*Stay
flexible.*

NEW Modular
4D Phantom

OCTAVIUS 4D

4D Patient and Machine QA



- ▶ Patient and machine QA with one single system
- ▶ Modular – various detector arrays and phantom tops
- ▶ Truly isotropic 3D dose verification
- ▶ Patient-based DVH analysis, entirely independent of the TPS
- ▶ Fast, independent point dose calculation with optional DIAMOND® software

PTVW

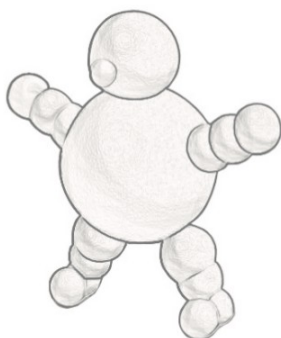
*Knowing what
responsibility means*

WWW.OCTAVIUS4D.COM USA | LATIN AMERICA | CHINA | ASIA PACIFIC | INDIA | UK | FRANCE | IBERIA | GERMANY



Confidence
Consistency
Efficiency

RAPIDPLAN™ – KNOWLEDGE-BASED PLANNING



RapidPlan™ knowledge-based planning opens the door to the next generation of individualized treatment planning by giving clinicians the confidence to treat a wide range of cancer types using knowledge-based planning.

By providing access to pre-configured plan models, RapidPlan may help clinics reduce variability in treatment planning to achieve greater consistency, efficiency and quality in patient care.

Streamline your planning process!

